Faculty Papers and Publications in Animal Science

Animal Science Department

2019

# Yes-associated protein 1 is required for proliferation and function of bovine granulosa cells in vitro

Michele R. Plewes

Xiaoying Hou

Pan Zhang

Aixin Liang

Guohua Hua

*See next page for additional authors*

## Authors

Michele R. Plewes, Xiaoying Hou, Pan Zhang, Aixin Liang, Guohua Hua, Jennifer R. Wood, Andrea S. Cupp, Xiangmin Lv, Cheng Wang, and John S. Davis

Research Article

# Yes-associated protein 1 is required for proliferation and function of bovine granulosa cells in vitro[†]

**Michele R. Plewes[1,2], Xiaoying Hou[1], Pan Zhang[1], Aixin Liang[1,3], Guohua Hua[1,3], Jennifer R. Wood[4], Andrea S. Cupp[4], Xiangmin Lv[1], Cheng Wang[1] and John S. Davis[1,2,*]**

[1]Department of Obstetrics and Gynecology, Olson Center for Women's Health, University of Nebraska Medical Center, Omaha, NE, USA [2]Veterans Affairs Nebraska Western Iowa Health Care System, Omaha, NE, USA [3]College of Animal Science and Technology, Huazhong Agricultural University, Wuhan, China [4]Department of Animal Sciences, University of Nebraska–Lincoln, Lincoln, NE, USA

*Correspondence: Olson Center for Women's Health, University of Nebraska Medical Center, 983255 Nebraska Medical Center, Omaha, NE 68198-3255, USA. Tel: 402 559-9079; Fax: 402 559-5015; E-mail: jsdavis@unmc.edu

[†]Grant Support: This project was supported by Agriculture and Food Research Initiative Competitive Grant no. 2017-67015-26450 to JSD and 2018-67012-29531 to MRP from the USDA National Institute of Food and Agriculture; NIH grants R01 HD087402, R01HD092263, and P01AG029531; the Department of Veterans Affairs IBX004272; and The Olson Center for Women's Health.

Received 25 January 2019; Revised 28 May 2019; Accepted 25 June 2019

## Abstract

Yes-associated protein 1 (YAP1) is a major component of the Hippo signaling pathway. Although the exact extracellular signals that control the Hippo pathway are currently unknown, increasing evidence supports a critical role for the Hippo pathway in embryonic development, regulation of organ size, and carcinogenesis. Granulosa cells (GCs) within the ovarian follicle proliferate and produce steroids and growth factors, which facilitate the growth of follicle and maturation of the oocyte. We hypothesize that YAP1 plays a role in proliferation and estrogen secretion of GCs. In the current study, we examined the expression of the Hippo signaling pathway in bovine ovaries and determined whether it was important for GC proliferation and estrogen production. Mammalian STE20-like protein kinase 1 (MST1) and large tumor suppressor kinase 2 (LATS2) were identified as prominent upstream components of the Hippo pathway expressed in granulosa and theca cells of the follicle and large and small cells of the corpus luteum. Immunohistochemistry revealed that YAP1 was localized to the nucleus of growing follicles. In vitro, nuclear localization of the downstream Hippo signaling effector proteins YAP1 and transcriptional co-activator with PDZ-binding motif (TAZ) was inversely correlated with GC density, with greater nuclear localization under conditions of low cell density. Treatment with verteporfin and siRNA targeting YAP1 or TAZ revealed a critical role for these transcriptional co-activators in GC proliferation. Furthermore, knockdown of YAP1 in GCs inhibited follicle-stimulating hormone (FSH)-induced estradiol biosynthesis. The data indicate that Hippo pathway transcription co-activators YAP1/TAZ play an important role in GC proliferation and estradiol synthesis, two processes necessary for maintaining normal follicle development.

## Summary Sentence

Hippo pathway transcription coactivators YAP1/TAZ play an important role in bovine granulosa cell proliferation and estradiol synthesis.

## Introduction

The ovary is a dynamic reproductive endocrine organ responsible for producing the ovum and providing sex steroids that are required for female fertility and quality of life. The growth and development of ovarian follicles require a series of coordinated events that induce morphological and functional changes within the follicle; specifically, promoting somatic cell growth and differentiation and oocyte maturation. Granulosa cells (GCs) undergo dramatic morphological and physiological changes throughout follicular growth and atresia, ovulation, and luteinization [1, 2]. Granulosa cells are responsible for the production of sex steroids, enzymes, growth factors, and cytokines required for a successful pregnancy. In mammals, follicle-stimulating hormone (FSH) released from the anterior pituitary gland, binds to receptors on GCs and stimulates the expression of cytochrome P450 family 19 subfamily A member 1 (CYP19A1), an enzyme responsible for estradiol biosynthesis [3], which promotes oogenesis and follicular development. During the estrous cycle, GC proliferation and apoptosis are tightly controlled and synchronized [4, 5]. Transforming growth factor-alpha (TGFα), a potent mitogen, stimulates GC proliferation by inducing critical regulators of cell growth and migration [6]. However, despite decades of extensive research, the molecular mechanisms governing GC proliferation and apoptosis remain unclear.

The Hippo signaling pathway (also referred to as the Salvador/Warts/Hippo pathway) is highly conserved and plays a critical role in maintaining tissue homeostasis by regulating both cell proliferation and apoptosis in various species [7, 8]. This signaling pathway consists of several negative regulators acting in a kinase cascade that ultimately phosphorylate and inactivate the transcriptional co-activators, Yes-associated protein 1 (YAP1) and transcriptional co-activator with PDZ-binding motif (TAZ) (also called WW domain containing transcription regulator 1 [WWTR1]) [9]. The core kinase cascade of the Hippo pathway consists of upstream Ste20-like protein kinases (serine/threonine kinase [STKs]) (commonly known as MST1/2) and the large tumor suppressor kinases 1/2 (LATS1/2) [10]. MST1/2 serine/threonine kinase activity is enhanced by interaction with the salvador family WW domain containing protein 1 (SAV1) scaffold protein. MST1/2 kinases and SAV1 form a complex to phosphorylate and activate LATS1/2 [11]. Phosphorylated LATS1/2 in complex with its regulatory protein MOB kinase activator 1 (MOB1) phosphorylates and inhibits downstream effector proteins, YAP1 and TAZ. In the phosphorylated state (inactive), YAP1 and TAZ are generally associated with 14-3-3 proteins in the cytoplasm and ultimately targeted for degradation [12]. When Hippo signaling is inactivated, levels of non-phosphorylated YAP1/TAZ increase, allowing for their accumulation in the nucleus; however, the mechanism is not fully understood. Following nuclear import, YAP1 and TAZ bind with TEA domain transcription factors (TEAD), which induce expression of genes that promote cell proliferation and inhibit apoptosis [13]. The Hippo signaling cascade is regulated by numerous upstream signals which include G-protein coupled receptors [14], Wnt signaling [15], mechanical stress [16, 17], cell polarity [18], as well as

microRNAs [19]. YAP1 and TAZ have been found to interact with different signaling pathways, such as Wnt, TGFβ, Notch, and IGF [20]; each of which is known to contribute to follicle development and ovarian function.

Recent studies indicate that the Hippo signaling pathway may play an important role in regulating mammalian ovarian physiology and pathology [21, 22]. The major components of the Hippo signaling cascade were found to be spatially and temporally expressed in the mouse ovary [23]; with reduced levels of messenger RNA (mRNA) and protein for MST and LATS and increased levels of YAP1 in proliferating GCs. Interestingly, YAP1 was predominantly cytoplasmic, whereas TAZ was nuclear in somatic cells [24], indicating that YAP1 and TAZ may be differentially regulated and have different functions in the ovary. A study in the chicken showed that the scaffold SAV1 played a suppressive role in follicle development by promoting the activity of LATS1 [25]. Ji et al. [26] provided evidence that androgen and estrogen treatment promote nuclear localization of YAP1 and that YAP1 is required for proliferation of mouse GCs. Studies by Kawamura et al. demonstrated that mechanical cues (i.e., fragmentation of the ovarian cortex) lead to suppression of Hippo signaling and thus an increase in nuclear localization of YAP1 in preantral follicles [27, 28]. This change resulted in the expression of YAP1 target genes cellular communication network growth factors 1 and 2 (CCN1/2, commonly known as CRY61 and CTGF, respectively), and baculoviral inhibitors of apoptosis repeat containing (BIRC) proteins and stimulation of secondary follicle growth. YAP1 is highly expressed in human GC tumors and knockdown or overexpression of YAP1 was directly linked to suppression or stimulation of cell proliferation [29]. These reports only begin to reveal the roles for each of the Hippo pathway components and how they are regulated during follicle development and differentiation.

Knockout studies in mice revealed that YAP1 deletion is embryonic lethal and *TAZ (Wwtr1)* deletion results in viable mice with kidney defects [30]. Mice deficient in *Lats1* exhibit an increase in germ cell apoptosis, develop follicular cysts and ovarian tumors and display marked infertility [24]. *Lats1* deficient mice also develop hyperplastic changes in the pituitary gland, which may disrupt the endocrine system. Studies in mice with germ cell-specific YAP1 knockouts demonstrated that YAP1 is not required for oogenesis or spermatogenesis [31]. Another study concluded that nuclear YAP1 does not play an important role in oocyte development [32]. Furthermore, the studies showed that oocyte-specific depletion of YAP1 does not alter ovarian follicle development but results in subfertility owing to poor oocyte quality leading to impaired early embryogenesis. A recent study in the bovine reported similar findings that inhibition of YAP1 activity, either by the small molecule YAP1 inhibitor, verteporfin, or by YAP1 targeting GapmeR antisense oligonucleotides, reduced the percent of zygotes that became blastocysts [33]. Collectively, the evidence points to a more prominent role for the Hippo pathway/YAP1 signaling in ovarian somatic cells than oocytes during follicle development.

The role of Hippo/YAP1 signaling in the bovine ovary is largely unknown. Understanding the influence of FSH and ovarian growth

factors, such as TGFα, on Hippo signaling in GCs may lead to a better understanding of the molecular mechanisms governing follicle growth. The current study examined the expression of Hippo signaling components in the bovine ovary and localization and possible roles of YAP1 and TAZ in GCs. The data indicate that these transcriptional co-activators play important roles in granulosa proliferation and estradiol synthesis.

## Materials and methods

### Ethics statement
The research conducted did not require animal protocol approval as the material was obtained from a slaughter house. this fact is indicated in the materials and methods section.

### Chemicals
Penicillin–streptomycin and Gentamycin were from Gibco (Gaithersburg, MD, USA), and Amphotericin B was from MP Biomedical, (Santa Ana, CA). Human FSH was from NHPP/NIDDK (Torrance, CA, USA). DMEM-F12 and M199 were from Invitrogen (Carlsbad, CA, USA). Fetal bovine serum (FBS) was from Atlanta Biologicals, Inc. (Lawrenceville, GA, USA). The SuperSignal West Femto Chemiluminescent Substrate Kit was from Pierce/Thermo Fisher Scientific (Rockford, IL, USA); Optitran Nitrocellular transfer membrane was from Schleicher & Schuell Bioscience (Dassel, Germany). Nuclear extraction kit was purchased from Active Motif (Carlsbad, CA, USA). 3,3-Diaminobenzidine (DAB) kit was from Invitrogen (Carlsbad, CA, USA). DAKO LSAB Kit was from Carpinteria, CA, USA). Mayer's hematoxylin and 3-(4,5-dimethylthiazol-2-yl)-2,5-diphenyltetrazolium bromide (MTT) were from Sigma-Aldrich (St. Louis, MO, USA). Yes-associated protein 1 small interfering RNA (siRNA) was from Dhamarcon/Thermo Scientific (Pittsburgh, PA, USA). [$^3$H] Thymidine was from MP Biomedicals LLC (Santa Ana, CA, USA). Fluoromount-G and clear nail polish were purchased from Electron Microscopy Sciences (Hatfield, PA, USA). Bio-Rad protein assay dye reagent concentrate is from Bio-Rad (Hercules, CA, USA).

All antibodies used in the study are found in Table 1. Biotin was added to phosphorylated YAP1 (Ser127) polyclonal antibody (Table 1) using a commercially available kit per manufacture's protocol (DSB-X Biotin Protein Labeling Kit; Cayman Chemical Company). In brief, the stock antibody solution was diluted to 0.5 mg/ml and desalted using a spin column prior to labeling. Two hundred microliters of desalted antibody was combined with 20 µl of freshly prepared 1 M $NaHCO_3$ and placed in a reaction tube. DSB-X biotin succinimidyl ester was reconstituted in 40 µl of dimethyl sulfoxide, and 2 µl of the DSB-X biotin solution was added to 200 µl of phosphorylated YAP1 (Ser127) polyclonal antibody. The derivatization reaction was carried out at room temperature for 1.5 h with constant stirring. The biotinylated antibody was collected using a spin column containing purification resin and centrifuged 5 min at $1100 \times g$ to remove unbound DSB-X. Labeling of antibody was verified using sodium dodecyl sulfate-polyacrylamide gel electrophoresis (SDS-PAGE) and western blotting (data not shown).

### Bovine granulosa cell isolation
Bovine GCs were isolated from follicles of increasing size (2–5, 5–10, and >10 mm) from ovaries collected at the local slaughterhouse. Briefly, GCs were collected by scraping and flushing the inner layers of follicles and washed twice in DMEM-F12. Freshly isolated GCs from follicles of increasing size were immediately processed for Western blot analysis.

Cell cultures were performed with GCs isolated from 2–5 mm follicles. Cells were then plated on a 60 $mm^2$ culture dish at 5 $\times 10^6$ cells/dish with culture media (DMEM-F12, 1 or 10% FBS, and 1× antibiotics) and maintained at 37 °C in an atmosphere of 95% humidified air and 5% $CO_2$, as described above until 80–85% confluent.

### Bovine luteal cell isolation
For comparison, some experiments were performed with bovine small luteal cells (SLCs). In brief, the corpus luteum was surgically dissected from the ovary and minced finely using a microtome and surgical scissors. Tissue pieces were dissociated using collagenase (103 U/ml) in the basal medium [M199 supplemented with antibiotics (100 U/ml penicillin G-sodium, 100 µg/ml streptomycin sulfate, and 10 µg/ml gentamicin sulfate)] for 45 min in spinner flasks at 37 °C. Following incubation, the supernatant was removed and transferred to a sterile 15 ml culture tube. Cells were then washed 3× with sterile PBS, resuspended in 10 ml of elutriation medium (calcium-free DMEM medium, 4.0 g/l glucose, antibiotics, 25 mM HEPES, 0.1% BSA, and 0.02 mg/ml deoxyribonuclease l; pH 7.2), and placed on ice. Fresh dissociation medium was added to the remaining undigested tissue and incubated with agitation for an additional 45 min. The remaining cells were collected, washed 2× with sterile PBS, and combined with the previous sample. After the final wash, cells were resuspended in 10 ml of culture medium. Viability of cells was determined using trypan blue and cell concentration was estimated using a hemocytometer prior to cell elutriation.

Freshly dissociated cells were resuspended in 30 ml elutriation medium. Dispersed luteal cells were enriched for SLCs and large luteal cells (LLCs) via centrifugal elutriation as previously described [34]. Cells with a diameter of 15–25 µm were classified as SLCs (purity > 90%).

### Immunohistochemistry
Bovine ovaries were collected during early pregnancy from a local slaughterhouse (JBS USA, Omaha, NE). Ovaries were fixed in 10% formalin for 24 h and then changed into 70% ethanol until embedded in paraffin. Tissues were cut into 4 µm sections and mounted onto polylysine-coated slides. Slides were deparaffinized through three changes of xylene and through graded alcohols to water and microwaved in unmasking solution (Vector H-3300) for antigen retrieval. Endogenous peroxidase was quenched with 0.3% hydrogen peroxide in methanol for 30 min. Sections were incubated with anti-YAP1, anti-phosphoYAP1, or anti-TAZ as indicated in Table 1 and subsequently an anti-rabbit ABC (Vector PK-4001) and stained using a DAB detection kit (Vector SK-4100). Slides were counterstained with Mayer's hematoxylin, dehydrated through graded alcohols, and mounted with Fluoromount-G. Nonimmune IgG from the host species was used as a control.

### Subcellular fractionation
Cytoplasmic and nuclear fractions of cultured GCs ($2.5 \times 10^6$) isolated from 2–5 mm follicles and SLCs ($2.5 \times 10^6$) were prepared following the manufacture's instruction. Nuclear and cytoplasmic proteins (20 µg) were analyzed by SDS-PAGE and western blot analysis.

**Table 1.** Characteristics of antibodies used for western blotting and microscopy.

| Antibody name | Dilution ratio | Species specificity | Source | Supplier (distributor, town, and country) | Cat. No |
|---|---|---|---|---|---|
| YAP1 | 1:400[1]/1:1000[2]/1:200[3] | Mouse | Rabbit pAB | Cell Signaling (Boston, MA, USA) | 4912S |
| Phospho-YAP1 (Ser127) | 1:400[1]/1:1000[2]/1:200[3,4] | Mouse | Rabbit pAB | Cell Signaling | 4911S |
| TAZ | 1:400[1]/1:1000[2]/1:200[3] | Mouse | Rabbit pAB | Cell Signaling | 4883S |
| CYP19A | 1:1000 | Human | Rabbit pAB | Abcam (Cambridge, United Kingdom) | ab80206 |
| STAR | 1:10000 | Mouse | Rabbit pAB | Abcam | ab96637 |
| CYP11A1 | 1:1000 | Mouse | Rabbit mAB | Cell Signaling | 14217 |
| HSD3B | 1:1000 | Mouse | Mouse mAB | A gift from Dr. Ian Mason | |
| TOP2A | 1:1000 | | | CalBioChem (Emdmillipore; Burlington, MA, USA) | NA14 |
| NFKB1A | 1:1000 | Mouse | Rabbit pAB | Abcam | ab86299 |
| Cyclin D1 | 1:1000 | Mouse | Rabbit mAB | Cell Signaling | 2978 |
| ACTB | 1:5000 | Bovine | Mouse mAB | Sigma Life Science (St. Louis, Missouri, USA) | A5441 |
| Alpha-tubulin | 1:200 | Bovine | Mouse mAB | Abcam | ab7291 |
| HRP-linked | 1:10000 | Anti-rabbit | | Jackson ImmunoResearch (West Grove, PA, USA | 111035003 |
| HRP-linked | 1:10000 | Anti-mouse | | Jackson Laboratory | 115035205 |
| DAPI[5] | 300 nM | | | Thermo Fisher (Carlsbad, CA, USA) | D1306 |
| Alexa Fluor 488 | 1:500 | Anti-mouse | | Invitrogen (Carlsbad, CA, USA) | A32723 |
| Alexa Fluor 594 | 1:500 | Anti-rabbit | | Invitrogen | A-11032 |
| Alexa Fluor 647 | 1:500 | Anti-biotin | | Biolegend (San Diego, CA, USA) | 405237 |

[1]Diltuion used for immunohistochemistry.
[2]Diltuion used for Western blotting.
[3]Diltuion used for confocal microscopy.
[4]Biotinylated antibody.
[5]DAPI, 4 4′,6-diamidino-2-phenylindole.
YAP1, Yes-associated protein 1; TAZ, WWTR1, WW domain containing transcription regulator 1; CYP19A1, aromatase; STAR, steroidogenic acute regulatory protein; HSD3B, 3 beta-hydroxysteroid dehydrogenase; CYP11A1, cholesterol side-chain cleavage enzyme; TOP2A, nuclear protein: DNA topoisomerase II alpha; cytosolic protein NFKB1A, nuclear factor of kappa light polypeptide gene enhancer in B-cells 1; ACTB, beta-actin (loading control).

## Western blot analysis

Freshly isolated and cultured bovine GCs were harvested with ice-cold cell lysis buffer (20 mM Tris-HCl (pH = 7), 150 mM NaCl, 1 mM Na2EDTA, 1 mM EGTA, 1% Triton X-100 and protease and phosphatase inhibitor cocktails). The lysed cells were sonicated and cleared by centrifugation at $14\,000\times g$ for 5 min. Protein content was determined using a Bio-Rad protein assay kit. The cell lysates (40–60 µg protein per lane) were subjected to 10% SDS-PAGE and transferred to nitrocellulose membranes as described previously [35]. The membranes were blocked within PBS with 5% BSA and blotted with primary dilutions and HRP-conjugated secondary antibodies dilutions as listed in Table 1. Signals were detected using Thermo Scientific SuperSignal West Femto Chemiluminescent Substrate Kit. The images were captured and analyzed with a UVP gel documentation system (UVP, Upland, CA, USA).

## Yes-associated protein 1 and TAZ knockdown

Yes-associated protein 1 and TAZ knockdown was achieved using siYAP1 (E-012200-02005) and siTAZ (E-016083-00-005) purchased from Dharmacon. siGLO (a cy5-labeled non-targeting siRNA as control) from Dharmacon was used as a control. Cells were transfected with either siGLO, siYAP1, or siTAZ for 6 h using Metafectene (Biontex-USA, San Diego, CA) according to the manufacturer's instruction. Cells were maintained at 37 °C in an atmosphere of 95% humidified air and 5% $CO_2$ for 48-h prior to use in studies for cell proliferation or estrogen production.

## Cell proliferation assays

Cells were harvested 72 h after siRNA transfection for determination of protein levels or cell numbers. Yes-associated protein 1 expression was determined by Western blot analysis and the cell numbers were quantified with an Invitrogen Countess automated cell counter (Carlsbad, CA, USA).

Granulosa cells were plated in 24-well plates at a density of $3 \times 10^4$ cells/well in DMEM-F12 with 10% FBS. After 24 h, cells were rinsed with PBS and incubated in DMEM-F12 with 2% FBS for 2 h. In some experiments, cells were treated with verteporfin, a selective YAP1 inhibitor, with or without TGFα (100 ng/ml) for 24 h. In other experiments, cells were treated with control siRNA, siYAP1 or siTAZ for 48 h prior to 24 h treatment with or without TGFα. [$^3$H] Thymidine (4 µCi/ml) was added 4 h before the end of the incubation period. Unincorporated radioactivity was removed by washing cells with ice-cold PBS twice followed by the addition of 10% trichloroacetic acid for 10 min at 4 °C. Cells were then washed with ice-cold TCA and solubilized with 0.2 M NaOH/0.1% SDS at room temperature. The extract was neutralized with an equal volume of 1 N HCL. [$^3$H] Thymidine incorporation was determined by liquid scintillation counting.

## 17 Beta-estradiol enzyme-linked immunosorbent assay

Bovine GCs were treated with siGlo (siCTL) or siYAP1 as described above. Granulosa cells were cultured in Dulbecco modified eagle's medium (DMEM)-F12 supplemented with 2% FBS and 200 nM 4-androstene-3 17-dione and then treated without (control) or FSH

(30 ng/ml) for 48 h. Conditioned media were collected for 17β-estradiol determination using an Estradiol EIA kit (Cayman Chemical Company, Ann Arbor, MI) according to the manufacturer's instructions.

## Microscopy and analysis

Granulosa cells were seeded at increasing cell densities of 0.125, 0.25, and $0.50 \times 10^6$ cells/well on glass coverslips ($22 \times 22$ mm No.1 thickness) in six-well culture dishes (9 cm$^2$ per well) to determine how cell contact/density influenced the localization of YAP1 and TAZ. Following plating, the cultures were maintained for 24 h at 37 °C in an atmosphere of 95% humidified air and 5% $CO_2$. Cells were then fixed with 200 µl of 4% paraformaldehyde and incubated at 4 °C for 30 min. Cells were rinsed 3× with 1 ml PBS following fixation. Cells were incubated with 200 µl of 0.1% Triton-X in 1× PBS at room temperature for 10 min to permeabilize the membranes. Cells were then rinsed 3× with 1 ml PBS and blocked in 1% BSA in PBS for 1 h at room temperature. Cells were rinsed 3× with 1 ml PBS prior to addition of YAP1 (1:200), phosphorylated YAP1 (Ser127; 1:200), TAZ (1:200), or alpha-tubulin (1:200) antibody for 1 h at room temperature. Following incubation, cells were washed 3× with PBS to remove unbound antibody and incubated with appropriate secondary antibodies at room temperature for 1 h. Cells were rinsed 3× with 1 ml PBS to remove unbound antibody. Following labeling with antibodies, coverslips containing labeled cells were mounted to glass microscope slides using 10 µl ProLong Gold Antifade Mountant with DAPI. Coverslips were sealed to glass microscope slides using clear nail polish and stored at −22 °C until imaging.

Images were collected using a Zeiss confocal microscope equipped with a 63X oil immersion objective (1.4 N.A) and acquisition image size of $512 \times 512$ pixel (33.3 µm × 33.3 µm). The appropriate filters were used to excite each fluorophore and emission of light was collected between 402 to 1000 nm. Approximately 30 cells were randomly selected from each slide and 0.33 µm slice z-stacked images were generated from bottom to top of each cell. A 3D image of each cell was created, and the area of an individual cell was generated using Zen software. Cells were then converted to maximum intensity projections and processed utilizing ImageJ (National Institutes of Health) analysis software. The JACoP plug-in was used in Image J software to determine the Manders' overlap coefficient for each image as previously described [36] and transformed into percent colocalization by multiplying Manders' overlap coefficient by 100.

## Expression of bovine Hippo pathway components

We mined bovine gene expression arrays from NCBI GEO repository (GSE83524) to analyze expression of Hippo signaling pathway components in freshly isolated bovine GCs (GC, $n = 4$) and theca cells (TCs) ($n = 3$) from large follicles and from purified preparations of bovine SLCs ($n = 3$) and LLCs ($n = 3$) from mature corpora lutea. Details of the isolation and analysis were previously published [37, 38]. Significant differences were identified as changes greater than 1.5-fold between GC and LLC or between TC and SLC, which were supported by unpaired *t*-tests with $P < 0.01$. Levels of beta-actin (*ACTB*) mRNA were not significantly different among cell types. When all cells types were combined as a group the relative expression of *ACTB* mRNA was 7845 ± 164, mean ± SEM.

## Statistical analysis

Each experiment was performed at least three times each using cell preparations from separate animals and dates of collection. All data are presented as means ± SEM. The differences in means were analyzed by one-way analysis of variance (ANOVA) followed by Tukey's multiple comparison tests to evaluate multiple responses, or by *t*-tests to evaluate paired responses. Welch's correction for unpaired *t*-tests was used when variances were significantly different. Two-way ANOVA was used to evaluate repeated measures with Bonferroni posttests to compare means. P values $\leq 0.05$ were considered significant unless otherwise indicated. All statistical analysis was performed using GraphPad Prism software from GraphPad Software, Inc.

## Results

### Expression and localization of Hippo signaling components in the bovine ovary

We mined bovine gene expression arrays from the NCBI GEO repository (GSE83524) for expression of key components of the Hippo signaling pathway [37, 38]. Figure 1A shows relative mRNA expression of *MST1/2*, *SAV1*, *LATS1/2*, *MOB1*, *YAP1*, and *TAZ* in bovine GCs and TCs (open blue symbols) and their luteal cell counterparts, LLCs and SLCs, respectively (closed red symbols). Levels of mRNA expression for *MST1, MST2, LATS2, MOB1A, and YAP1* were not different among all cell types. When all cell types were analyzed as a group the average levels of *MST*2 mRNA were 3–4-fold greater than *MST1* and the average levels of *LATS1* mRNA were 4–5-fold greater than *LATS2* mRNA (Figure 1B). Levels of *SAV1* and *TAZ* were increased (1.6- and 7.5-fold, respectively) in LLCs compared to GCs; whereas there was a 40% reduction *LATS1* transcripts in LLCs compared to GCs. Levels of *SAV1* transcripts in SLCs increased 2.4-fold compared to TCs.

The presence of YAP1 and TAZ proteins in bovine ovaries was determined using Immunohistochemistry (Figure 2A). The subcellular localization of the Hippo signaling effectors YAP1 and TAZ provides useful information regarding the possible role of YAP1 and TAZ in cellular responses. When Hippo signaling is active, YAP1 and TAZ are phosphorylated and shuttled from the nucleus to the cytoplasm, thus preventing their function as transcriptional coactivators [9]. YAP1 was prominently expressed in the granulosa layer of developing antral follicles; while staining in the theca layer was less intense and was further reduced in the stroma (Figure 2A, panel b). Although YAP1 was present in the cytoplasm, more intense staining was observed in the nuclei of GCs and TCs. Staining for phosphorylated YAP1 (Ser127) revealed a cytoplasmic distribution in both GCs and TCs (Figure 2A, panel c). In the corpus luteum, YAP1 was present in the cytoplasm and nucleus (Figure 2A, panel d). YAP1 staining was also observed in microvascular endothelial cells of the corpus luteum (arrows). TAZ immunostaining in antral follicles was more prominent in TCs compared to GCs (Figure 2A, panel g). TAZ was also present in the nucleus and cytoplasm throughout the corpus luteum, with a population of LLCs staining intensely. Staining was also evident in microvascular endothelial cells (Figure 2A, panel h).

We used Western blot analysis to evaluate YAP1 and TAZ expression in freshly isolated bovine GCs from follicles of various sizes (2 to >10 mm) and LLCs or SLCs (Figure 2B). Yes-associated protein 1 was expressed in GCs at all stages of follicle development and in SLCs and LLCs. Compared to small follicles the YAP1/ACTB
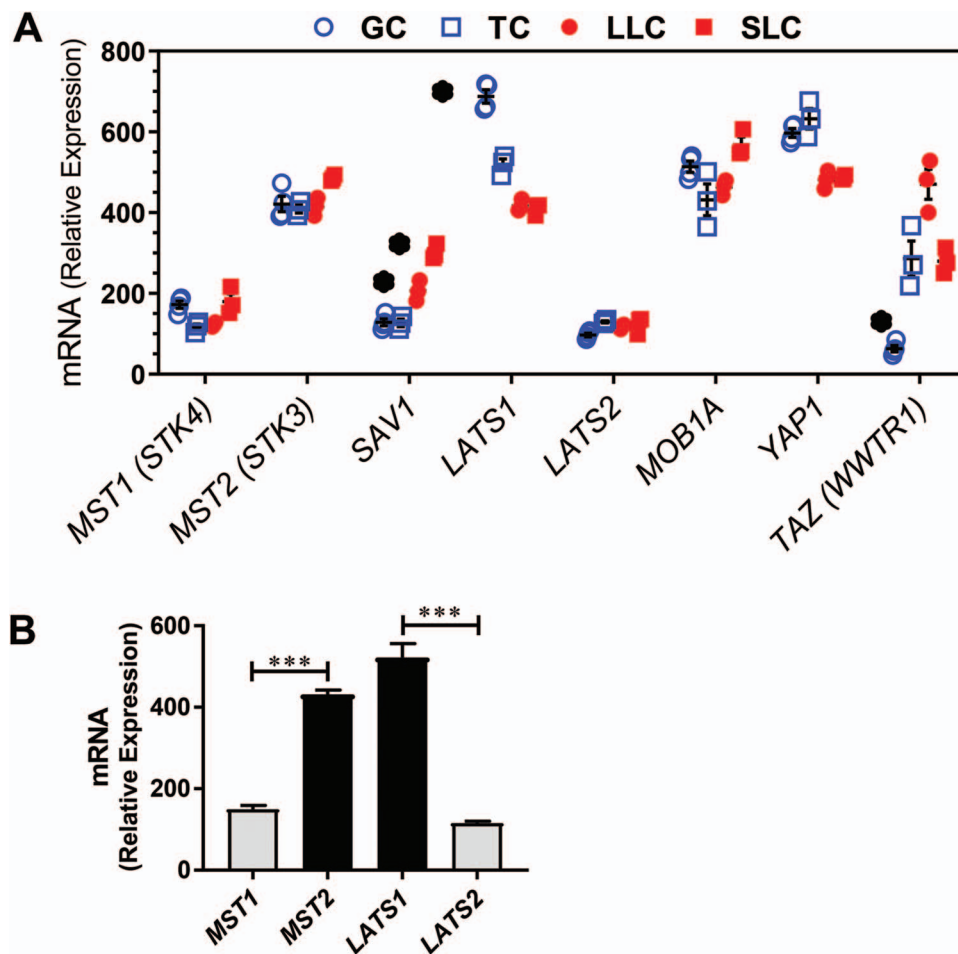
**Figure 1.** Expression of Hippo signaling family members in the bovine ovary. Microarray analysis was used to determine the expression of Hippo signaling family members in bovine follicular (theca and granulosa) and luteal (small and large) cells. (A) Microarray analysis of Hippo signaling family members in bovine GCs ($n = 4$; open blue circle), TCs ($n = 3$; open blue box), SLCs ($n = 3$; closed red box) and LLCs ($n = 3$; closed red circle). Relative mRNA units are shown as symbols with means ± SEM shown as black lines, in some cases, the black lines are obscured by the symbols. Significant differences were identified as changes greater than 1.5-fold and supported by unpaired $t$-tests with $P < 0.01$. *Significant difference between GC and LLC or TC and SLC. Serine/threonine kinase 4 (*STK4; MST1*); serine/threonine kinase 3 (*STK3, MST2*); salvador family WW domain containing protein 1 (*SAV1*); large tumor suppressor kinase 1 (*LATS1*); large tumor suppressor kinase 2 (*LATS2*); MOB kinase activator 1A (*MOB1A*); Yes-associated protein 1 (*YAP1*); WW domain containing transcription regulator 1 (*TAZ; WWTR1*); and beta-actin (*ACTB*). (B) Comparison of the expression of *MST1* versus *MST2* and *LATS1* versus *LATS2*. Levels of mRNA for each transcript in GC, TC, SLC, and LLC were pooled and analyzed as a single group. Data are means ± SEM. Differences in means in *MST1* versus *MST2* and *LATS1* versus *LATS2* were compared by $t$-test. ***$P < 0.001$.

ratio slightly increased by 14 ± 9% and decreased 23 ± 9% in 5–10 and >10 mm follicles, respectively (mean ± SEM, $n = 8$). In contrast, the expression of TAZ in GCs decreased with increasing follicle size. Compared to small follicles the TAZ/ACTB ratio decreased by 33 ± 10% and 59 ± 7% in 5–10 and >10 mm follicles, respectively (mean ± SEM, $n = 9$). However, TAZ was expressed in both SLCs and LLCs. Aromatase protein (CYP19A1) was detected only in GCs, whereas Steroidogenic acute regulatory protein (STAR) protein was detected in luteal cells (Figure 2B). Levels of 3β-hydroxysteroid dehydrogenase (3BHSD) and cholesterol side-chain cleavage enzyme (CYP11A1) increased with differentiation to luteal cells (Figure 2B).

Cellular fractions of cultured cells were prepared to determine the subcellular localization of YAP1 and TAZ in GCs from 2–5 mm follicles and SLCs. In GCs, greater levels of YAP1 and TAZ were present in the cytoplasm compared to the nucleus ($P < 0.05$; Figure 3). In cultures of luteal cells, YAP1 was evenly distributed in the cytoplasmic and nuclear fractions (Figure 3A and B). In contrast, greater amounts of TAZ were distributed to the nuclear fractions than

cytoplasmic fractions in luteal cells ($P < 0.05$; Figure 3A and D). As expected, phosphorylated YAP1 (Ser127) was predominantly present (≥80%) in the cytoplasm compared to the nucleus in GCs and luteal cells ($P < 0.05$; Figure 3A and B).

## Effects of cell density on the localization of Yes-associated protein 1, phosphorylated YAP1 (Ser127), and TAZ in bovine granulosa cells

Mechanical and cell–cell interactions are known to regulate Hippo activity, with less nuclear localization of YAP1 at high cell density [39]. Experiments were conducted to determine how cell contact/density influences the localization of YAP1 and TAZ in bovine GCs. Using confocal microscopy, a density-dependent decrease in nuclear YAP1 localization was observed as shown with decreased colocalization with DAPI ($P > 0.05$; Figure 4). GCs seeded at the lowest density had 43.37% greater levels of YAP1 colocalized with DAPI than GCs plated at $0.50 \times 10^6$ cell/well ($P > 0.05$; Figure 4). Moreover, there was a density-dependent increase in YAP1
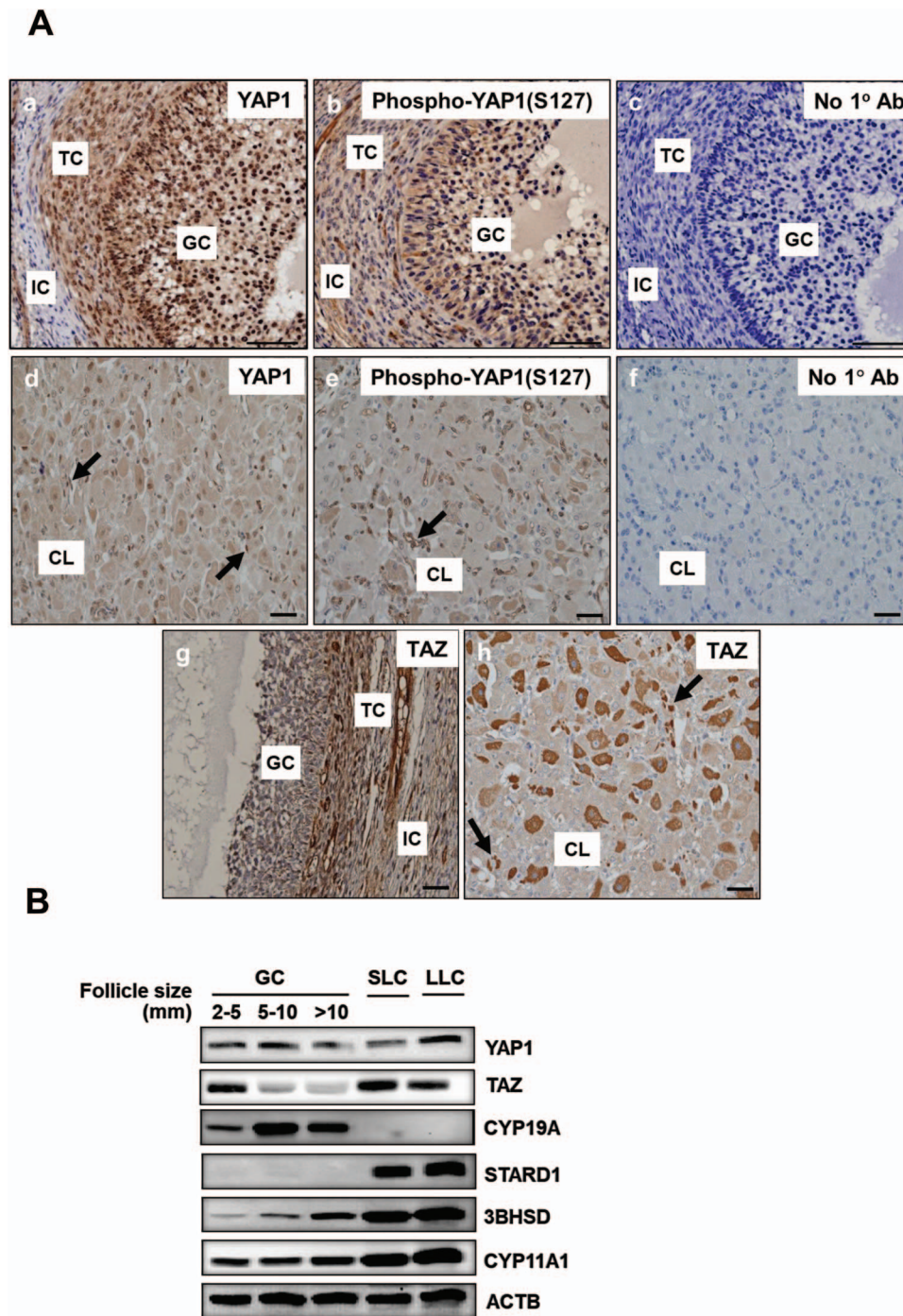
**Figure 2.** Localization of Hippo signaling family members in the bovine ovary. Immunohistochemistry and western blotting were used to determine the expression and localization of YAP1, phospho-YAP1(Ser127), and TAZ in bovine follicles and the corpus luteum. (A) Representative immunohistochemistry micrographs showing expression of YAP1 in GCs and TCs (b) and corpus luteum (d), phospho-YAP1(Ser127) in GC and TC (c) and corpus luteum (e); and TAZ in GC and TC (g) and corpus luteum (h). Micron bar represents 1 mm, negative controls (a and f). Large arrows point to luteal endothelial cells. (B) Western blot analysis of the expression of YAP1 and TAZ in GC from follicles of increasing size (2–5, 5–10, >10 mm) and enriched SLCs and LLCs. Expression of aromatase (CYP19A1), steroidogenic acute regulatory protein (STARD1), 3beta-Hydroxysteroid dehydrogenase (3BHSD), Cholesterol side-chain cleavage enzyme (CYP11A1), and Beta-actin (ACTB; loading control) are shown.

colocalization with alpha-tubulin observed ($P > 0.05$; Figure 4). Unlike total YAP1, there was no difference in colocalization of phosphorylated YAP1 (Ser127) with DAPI, regardless of cell density ($P < 0.05$; Figure 5). However, a density-dependent increase in phosphorylated YAP1 (Ser127) colocalization with alpha-

tubulin was observed ($P > 0.05$; Figure 5). Similar to the density-dependent changes in nuclear YAP1 localization, GCs plated at the lowest density had 33.4% more TAZ colocalized with DAPI when compared to GCs plated at the highest density ($P > 0.05$; Figure 6). Interestingly, there was a density-dependent decrease in the
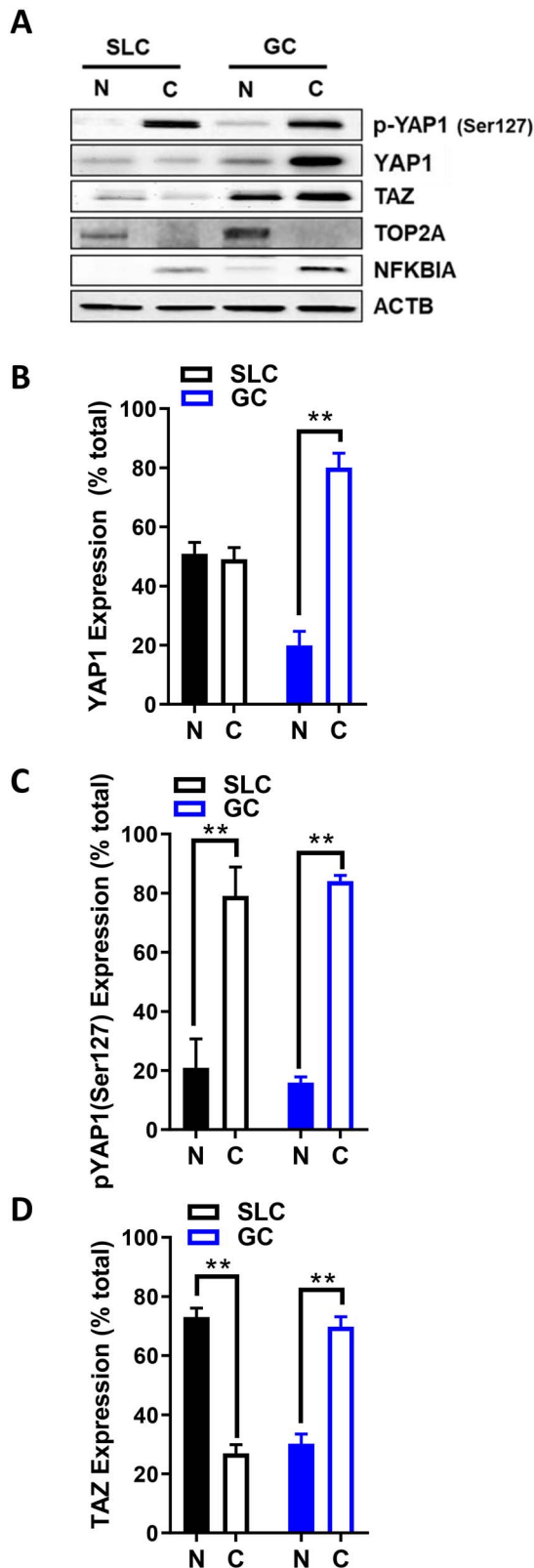
colocalizationh alpha-tubulin observed as cell density increased ($P > 0.05$; Figure 5).

## The Yes-associated protein 1 inhibitor verteporfin

### inhibits granulosa cell DNA synthesis

Experiments were performed in order to determine whether YAP1/TAZ had an impact on GC proliferation. To accomplish this, we used verteporfin, a small molecule that inhibits the association of the YAP1 with the transcription factor TEAD, which disrupts transcription and YAP1-mediated growth [40, 41]. GCs were treated with 5 µM verteporfin or vehicle control (M199) for 48 h in the presence or absence of FSH or TGFα, two factors that contribute to GCs survival and proliferation. Western blot analysis revealed that TGFα increased cyclin D1 protein $2.6 \pm 0.5$-fold (mean $\pm$ SEM, $n = 5$; $P < 0.05$) (Figure 7A and B) and increased DNA synthesis (Figure 7C). Pretreatment with verteporfin significantly reduced basal and TGFα-induced cyclin D1 protein levels. Treatment with 2.5 and 5 µM verteporfin also reduced basal as well as TGFα-induced DNA synthesis (Figure 7C). FSH did not increase cyclin D1 or stimulate bovine GC growth compared to vehicle-treated control cells ($P$; 0.05; Figure 5).

## Effects of knockdown of Yes-associated protein 1 and TAZ on transforming growth factor-alpha-induced proliferation in granulosa cells

In order to test whether YAP1 plays a role in cell proliferation, we transiently transfected bovine GCs with control siRNA targeting YAP1 (siYAP1) or Cy5-labeled Scramble siRNA (siGLO). Treatment with siYAP1 reduced YAP1 and phospho-YAP1 in control cells and cells treated with TGFα (Figure 8A and B). Treatment with siYAP1 significantly attenuated cell proliferation under basal conditions by 46% ($P < 0.05$, Figure 8C). Transforming growth factor-alpha (100 ng/ml) treatment for 48 h stimulated a 2.4-fold increase in GC proliferation ($P < 0.001$, Figure 8C). Knockdown of YAP1 inhibited the stimulatory effect of TGFα on GC proliferation ($P < 0.001$), Figure 8C).

Additional experiments were performed to determine whether TAZ also contributes to GC proliferation. Western blot analysis revealed that TAZ specific siRNA effectively reduced TAZ protein (Figure 8D) and significantly attenuated TGFα-induced cell proliferation (Figure 8E). Treatment with siRNA targeting both YAP1 and TAZ further reduced basal and TGFα-sFigure 8D and E).

## Effects of Yes-associated protein 1 on follicle-stimulating hormone-induced estradiol production in bovine granulosa cells

Granulosa cells uniquely produce estradiol for timing and control of the reproductive cycle. Here we show that FSH treatment significantly induced estradiol production by 7.6-fold in bovine GCs (Figure 9, $P < 0.001$). Treatment with siYAP1 knocked down YAP1 protein and significantly attenuated FSH-induced estradiol production by 80% (Figure 9, $P < 0.001$).
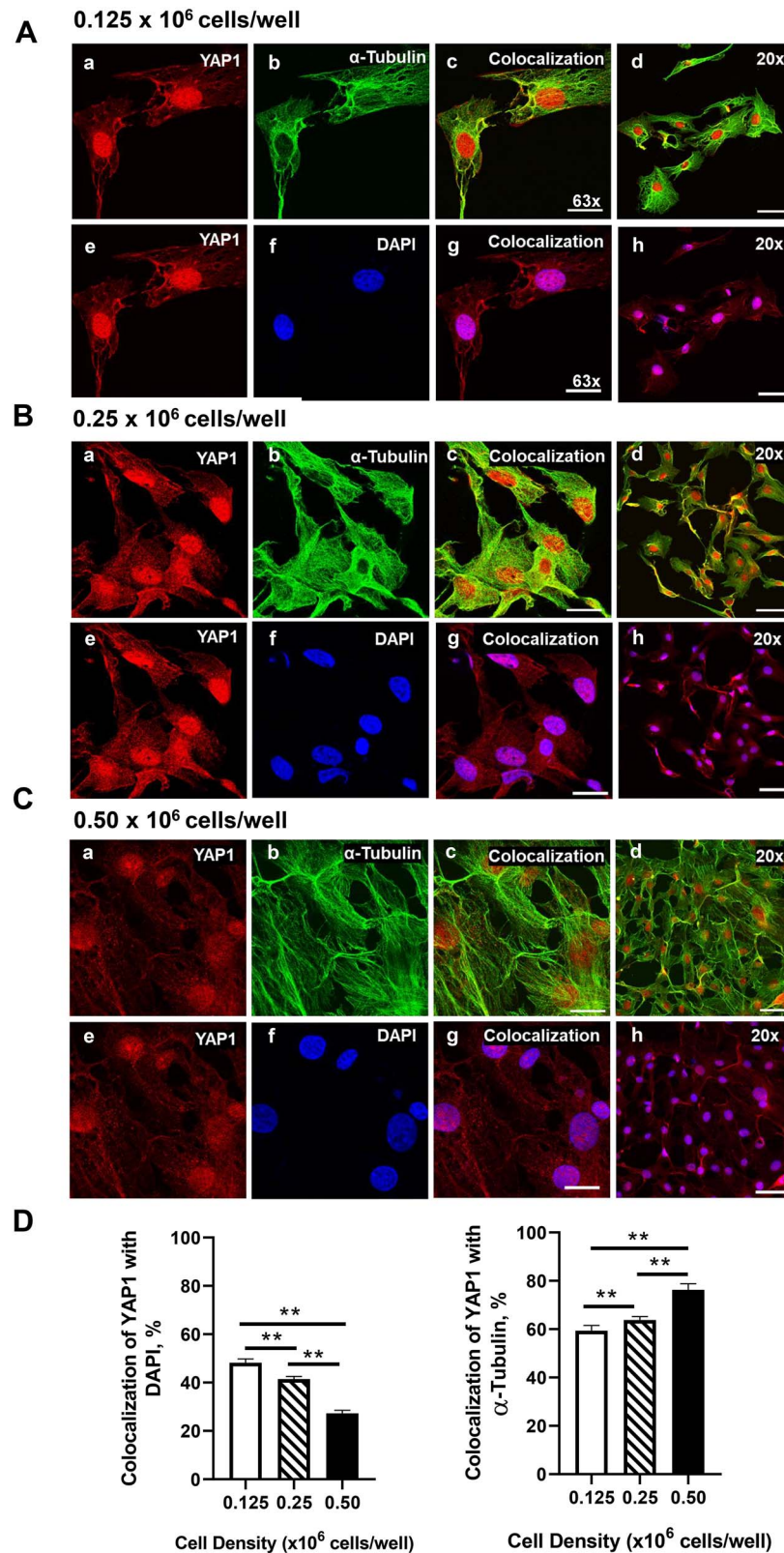
**Figure 3.** Expression of YAP1 and WW domain-containing transcription regulator 1 (TAZ; WWTR1) in the bovine ovary. Western blotting was used to determine the localization of YAP1, phospho-YAP1(Ser127), and TAZ in bovine follicles and the corpus luteum. (A) Representative western blots of YAP1, phospho-YAP1(Ser127) and TAZ in cytoplasmic and nuclear fractions obtained from cultured GC and enriched SLC. Nuclear protein: DNA topoisomerase II alpha (TOP2A); cytosolic protein: nuclear factor of kappa light polypeptide gene enhancer in B-cells 1 (NFKB1A); beta-actin (ACTB; loading control). (B–D) Densitometry of YAP1, phospho-YAP1(Ser127), and TAZ expression in nuclear and cytoplasmic fractions. Data represent the percentage of each protein within each fraction. Bars are means $\pm$ SEM, $n = 5$ experiments. ** $P < 0.01$.

**Figure 4.** Effects of cell density on nuclear localization of YAP1 in bovine GCs. Granulosa cells were seeded overnight on coverslips in six-well dishes at increasing cell densities from 0.125–0.50 × $10^6$ cells/well. (A) Representative micrograph of GC plated at 0.125 × $10^6$ cells/well; YAP1 (a), alpha-tubulin (b), colocalization of YAP1 and alpha-tubulin (c), 20× magnification of colocalization of YAP1 and alpha-tubulin (d), YAP1 (e), DAPI (e), colocalization of YAP1 and DAPI (g), 20× magnification of colocalization of YAP1 and alpha-tubulin (h). (B) Representative micrograph of GC plated at 0.25 × $10^6$ cells/well. (C) Representative micrograph of GC plated at 0.50 × $10^6$ cells/well. (D) Quantitative analysis of colocalization of YAP1 with alpha-tubulin and DAPI. Data are represented as means ± SEM, $n = 3$ experiments. **Significant difference as compared to 0.125 × $10^6$ cells/well, $P < 0.05$. Micron bar represents 20 μm (63×) and 50 μm (20×).
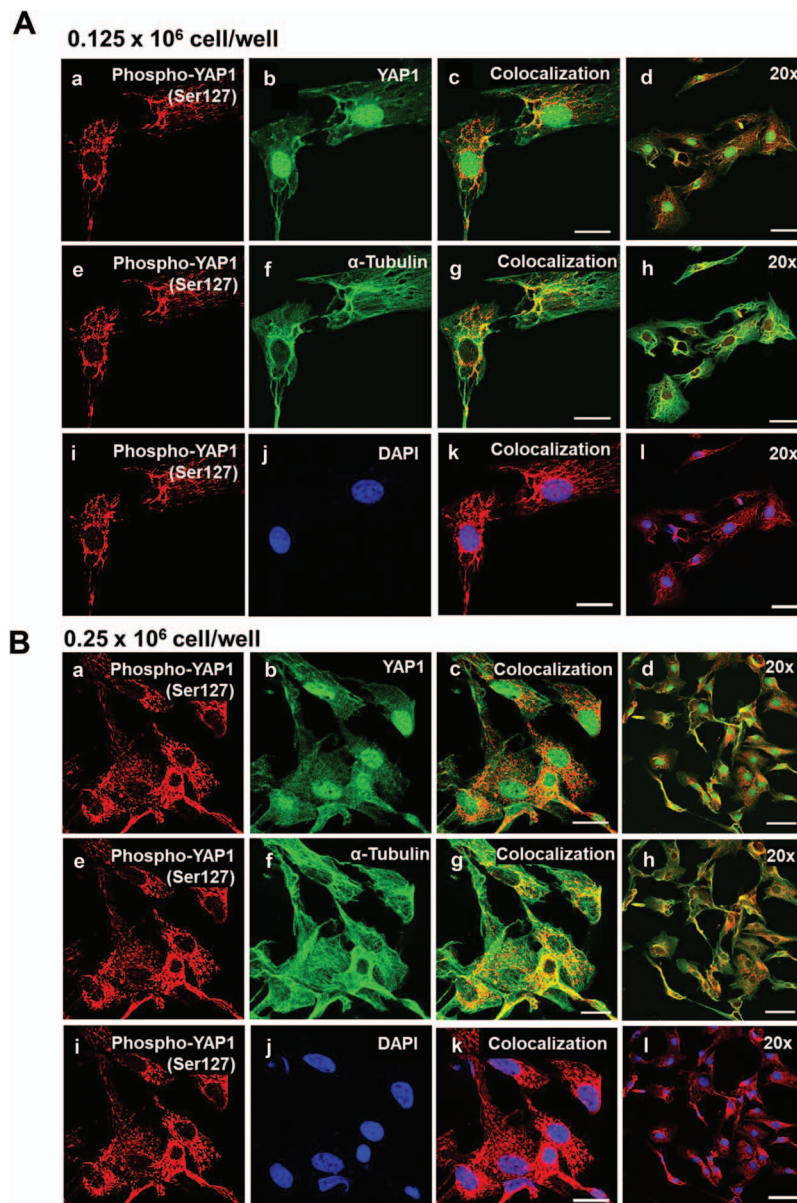
**Figure 5.** Effects of cell density on nuclear localization of phosphorylated YAP1 (Ser127) in bovine GCs. Granulosa cells were seeded overnight on coverslips in six-well dishes at increasing cell densities from 0.125 to 0.50 $\times$ $10^6$ cells/well. (A) Representative micrograph of GC plated at 0.125 $\times$ $10^6$ cells/well; phosphorylated Yes-associated protein (p-YAP1 (Ser127)) (a), YAP1 (b), colocalization of p-YAP1 (Ser127) and YAP1 (c), 20x magnification of colocalization of p-YAP1 (Ser127) and YAP1 (d), p-YAP1 (Ser127) (e), alpha-tubulin (f), colocalization of p-YAP1 (Ser127) and alpha-tubulin (g), 20$\times$ magnification of colocalization of p-YAP1 (Ser127) and alpha-tubulin (h), p-YAP1 (Ser127) (i), DAPI (j), colocalization of p-YAP1 (Ser127) and DAPI (k), 20$\times$ magnification of colocalization of p-YAP1 (Ser127) and alpha-tubulin (l). (B) Representative micrograph of GC plated at 0.25 $\times$ $10^6$ cells/well. (C) Representative micrograph of GC plated at 0.50 $\times$ $10^6$ cells/well. (D) Quantitative analysis of colocalization of p-YAP1 with YAP1, alpha-tubulin, and DAPI. Data are represented as means $\pm$ SEM, $n = 3$ experiments. **Significant difference as compared to 0.125 $\times$ $10^6$ cells/well, $P < 0.05$. Micron bar represents 20 μm (63$\times$) and 50 μm (20$\times$).

## Discussion

Recent studies provide evidence that the Hippo YAP1/TAZ signaling pathway in somatic cells of the ovary contributes to ovarian follicle development [24, 31, 32, 42]. The present study used a large animal model with similarities to human ovarian physiology [43] to better understand the expression and the potential roles of the Hippo pathway downstream effectors, YAP1 and TAZ, on two key aspects of follicle development, GC proliferation, and estrogen production. We observed that components of the Hippo signaling pathway are present in the bovine ovary and that

nuclear-localized downstream Hippo signaling effector proteins YAP1 and TAZ are present in growing bovine follicles and to a lesser extent in the fully differentiated corpus luteum. Furthermore, the nuclear localization of both YAP1 and TAZ was inversely correlated with cell density in primary cultures of GCs. We also observed that YAP1 and TAZ are required for GC proliferation and estrogen synthesis, two crucial processes during follicle development.

Examination of microarray studies of bovine theca and GCs and their luteal cell counterparts, SLCs and LLCs, respectively,
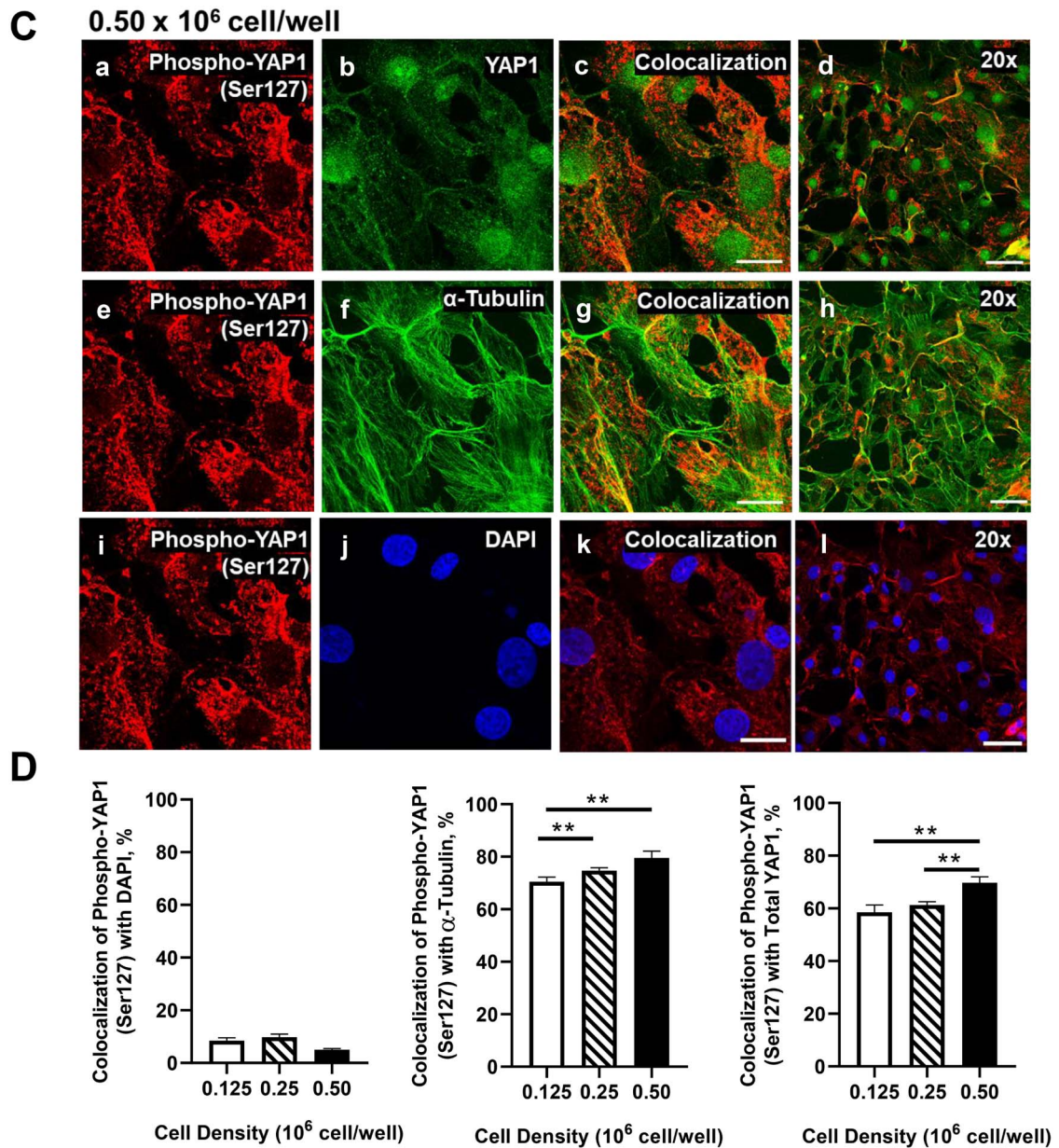
**Figure 5.** (Continued).

demonstrated that transcripts for key components of the Hippo signaling pathway are present in the bovine ovary. With few exceptions, transcript levels were unchanged with the differentiation of the follicular cells into luteal cells. A major exception was the MST scaffold protein SAV1, which was increased as theca and GCs differentiated in SLCs and LLCs. As an earlier study showed that SAV1 plays a suppressive role in follicle development by promoting the activity of LATS1 [25], the increase in SAV1 in luteal cells may contribute to active Hippo signaling and suppression of luteal cell proliferation. Also noted was a 7.5-fold increase in TAZ expression in LLCs compared to GCs from preovulatory follicles. The Hippo pathway effector proteins YAP1 and TAZ have been shown to have both distinct and overlapping functions [30, 44]. We speculate that the increase in TAZ expression may contribute to the increase in cell size rather than proliferation as GCs differentiate

into LLCs. Irrespective of cell type, the levels of *MST2* mRNA were 3–4-fold greater than *MST1*; and levels of *LATS1* mRNA were 4–5-fold greater than *LATS2* mRNA suggesting that MST2 and LATS1 form the main Hippo signaling kinase cassette in the bovine ovary.

Immunohistochemistry and Western blot analysis reveal that both YAP1 and TAZ are expressed in the cytoplasm and nucleus of bovine granulosa and TCs, as well as the corpus luteum. However, distinct cell-type-specific differences in YAP1 and TAZ are apparent; (1) YAP1 levels in GCs are relatively constant with follicle development and decline slightly in follicles greater than 10 mm; whereas, TAZ levels decrease with increasing follicle development, (2) TAZ is more prominent in theca layer, (3) levels of YAP1 protein is reduced in luteal cells compared to their follicular counterparts, (4) compared to YAP1, which is present in the cytoplasm and nucleus, TAZ is more
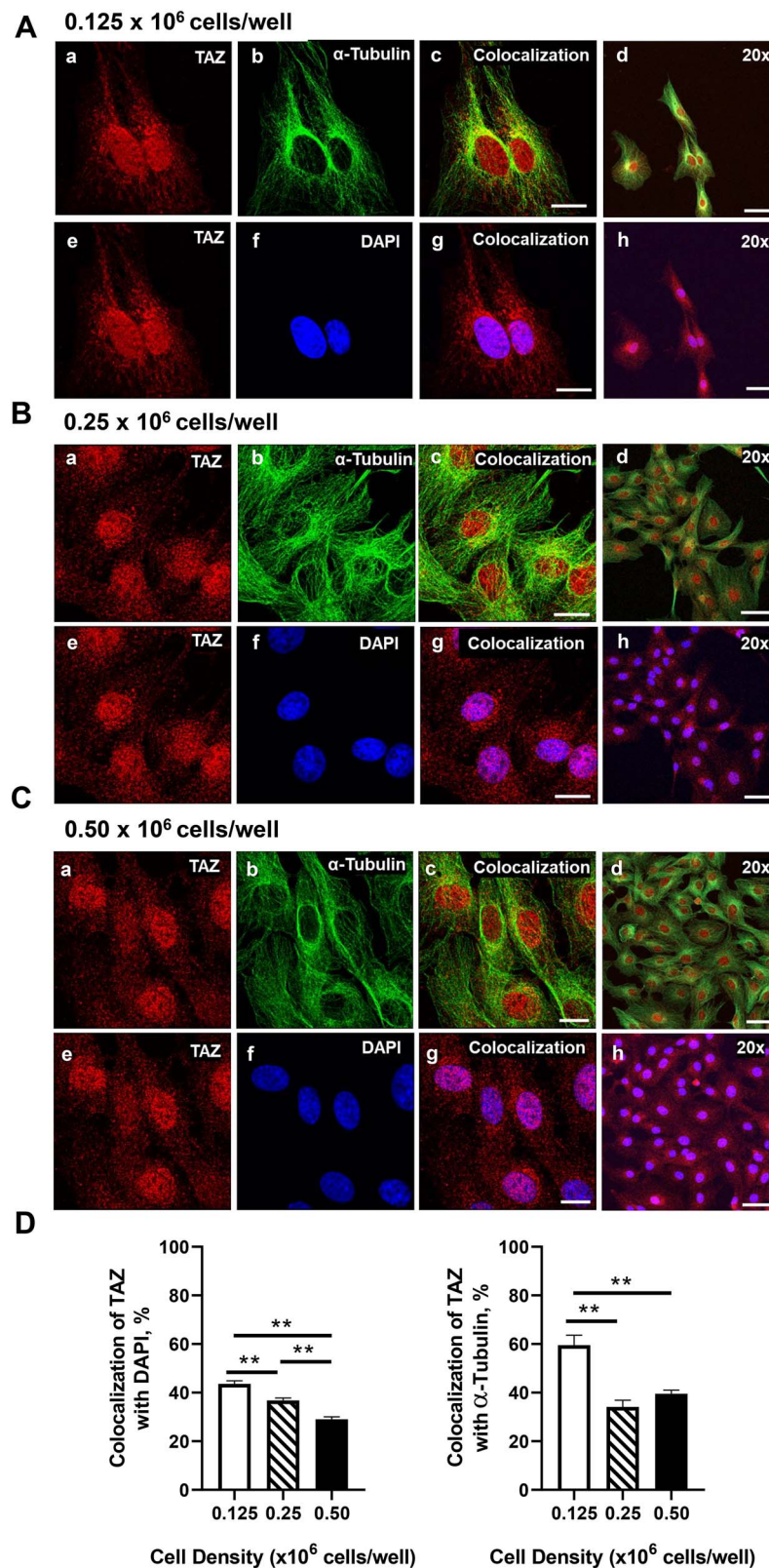
**Figure 6.** Effects of cell density on nuclear localization of TAZ in bovine GCs. Granulosa cells were seeded overnight on coverslips in 6-well dishes at increasing cell densities from 0.125–0.50 × $10^6$ cells/well. (A) Representative micrograph of GC plated at 0.125 × $10^6$ cells/well; WW domain-containing transcription regulator 1 (TAZ; WWTR1) (a), alpha-tubulin (b), colocalization of TAZ and alpha-tubulin (c), 20× magnification of colocalization of TAZ and alpha-tubulin (d), TAZ (e), DAPI (e), colocalization of TAZ and DAPI (g), 20× magnification of colocalization of TAZ and alpha-tubulin (h). (B) Representative micrograph of GC plated at 0.25 × $10^6$ cells/well. (C) Representative micrograph of GC plated at 0.50 × $10^6$ cells/well. (D) Quantitative analysis of colocalization of TAZ with alpha-tubulin and DAPI. Data are represented as means ± SEM, $n = 3$ experiments. **Significant difference as compared to 0.125 × $10^6$ cells/well, $P < 0.05$. Micron bar represents 20 μm (63×) and 50 μm (20×).
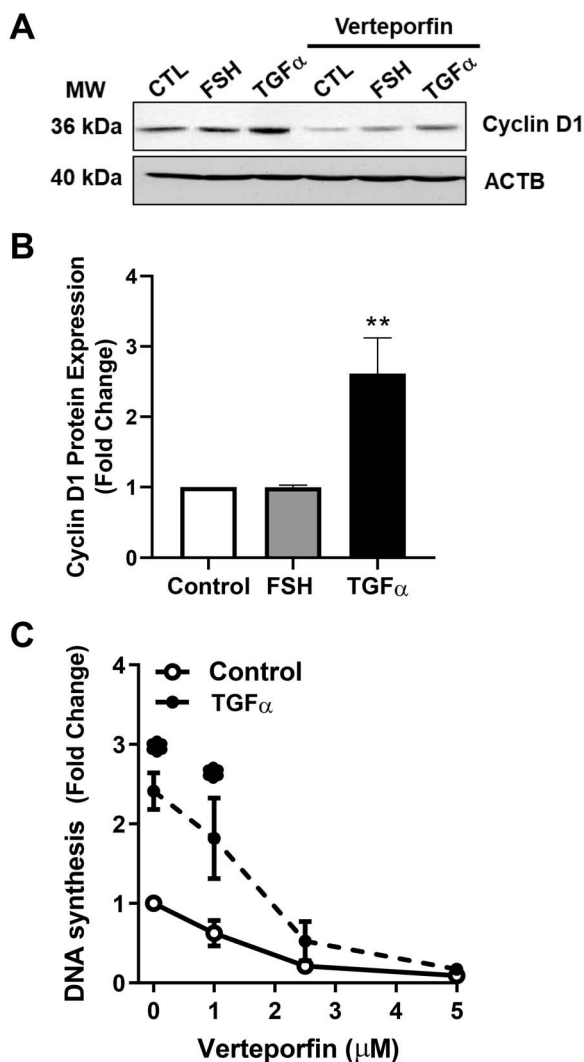
**Figure 7.** Effects of the YAP1 inhibitor verteporfin on GC proliferation. Bovine GC were plated at a cell density of $80 \times 10^3$ cells/well in 12-well dishes and treated with increasing concentrations of verteporfin (0–5 μM). Cell proliferation was determined as described in the Methods. (A) Representative western blot analysis showing Cyclin D1 expression in cells treated with follicle-stimulating hormone (30 ng/ml; FSH) or transforming growth factor-alpha (100 ng/ml; TGFα) in the presence or absence of verteporfin (5 μM). (B) Densitometry of cyclin D1 expression in cells treated with follicle-stimulating hormone (30 ng/mL; FSH) or transforming growth factor-alpha (100 ng/ml; TGFα). (C) DNA synthesis in cells treated with increasing concentrations of verteporfin (0, 1, 2.5. and 5 μM) following treatment of TGFα (100 ng/ml). Data are represented as means ± SEM ($n = 4$) of the average fold change from control in each experiment. **Significant difference as compared to control, $P < 0.05$.

prominent in the nucleus SLCs in vitro, (5) a TAZ immunostaining is high in a population of LLCs compared to other cells in the corpus luteum, and (6) YAP1 and TAZ are present in the microvascular endothelial cells of the corpus luteum. Cell type differences in YAP1 and TAZ are also observed in the developing mouse ovary where YAP1 is predominantly cytoplasmic, whereas TAZ is nuclear in somatic cells [24]. Collectively these findings (1) indicate that the cellular distribution of YAP1 and TAZ is differentially regulated in the bovine ovary, and (2) form a foundation, on which to unravel the roles of each of the Hippo pathway components during follicle development and corpus luteum formation.

Endothelial cells play an important role in the development [45] and regression [46] of the bovine corpus luteum. In addition to luteal steroidogenic cells, we observed immunostaining for YAP1 and TAZ in the microvascular endothelial cells of the corpus luteum. Although this intriguing observation awaits investigation, reports indicate that YAP1/TAZ is essential for vascular development and regression [47]. Endothelium-specific deletion of YAP1/TAZ leads to impaired vascularization and embryonic lethality [48]. Hippo-YAP1/TAZ signaling has also been implicated in the processes of endothelial cell sprouting and vessel maturation [49].

The Hippo pathway is variably regulated by cell contact and cell density [50, 51]. We seeded GCs at increasing cell densities to determine how cell contact/density influenced the cellular localization of YAP1 and TAZ in GCs. Using confocal microscopy, we observed that GCs seeded at the lowest density have the highest levels of YAP1 and TAZ in the nucleus. Our data demonstrating that cell density influences the localization of YAP1 and TAZ agrees with studies of other cell types [52–55]. Importantly, constitutive activation of YAP1 (nuclear-localized YAP1) can overcome cell–cell contact-induced cell growth inhibition [55]; implicating changing nuclear levels of YAP1/TAZ in achieving density-dependent control of cell proliferation and organ size. Other evidence supports the idea that alterations in tissue rigidity impact ovarian follicle growth (reviewed in [21, 56]). Studies by Kawamura et al. [28] demonstrated that fragmentation of human or murine ovaries facilitates the conversion of G-actin into F-actin, which disrupts ovarian Hippo signaling, leading to an increase in the expression of downstream growth factors, promotion of follicle growth, and the generation of mature oocytes [28]. The disruption of Hippo signaling, nuclear localization of YAP1 and promotion of follicle growth was also observed in response to drugs that promote actin polymerization [27]. The prominent nuclear localization of YAP1 observed in developing bovine follicles indicates that the expanding ovarian follicle does not provide an environment for mechanical cues or cell–cell contact-induced activation of Hippo signaling, which would reduce nuclear localization of YAP1 and limit follicle growth. Of clinical relevance, mechano-biological approaches (wedge resection, laser drilling, and use of ovarian fragments in vitro) have contributed to infertility treatments in patients with premature ovarian failure and polycystic ovary syndrome (PCOS), a common disorder in young women characterized by androgen excess and oligomenorrhea [21, 56]. These approaches presumptively inhibit Hippo signaling resulting in the activation of YAP1 leading to follicle activation [21].

Granulosa cell proliferation is critical for follicle development, ovum maturation and advancement of the reproductive cycle. Improper follicle development can result in delayed ovum maturation, failure to ovulate, and inadequate corpus luteum function [57]. Our results indicate that dysregulation of the Hippo/YAP1 signaling pathway inhibits proliferation of bovine GCs in vitro. In the follicle, ovarian TCs produce TGFα, which stimulates GC proliferation in many species including the bovine [58], monkey [59], mouse [60], and human granulosa-like tumor cells [29]. Treatment of GC cultures with verteporfin, a small molecule inhibitor that disrupts YAP1/TAZ activity by interrupting their interaction with the TEAD transcription factor [40, 61], inhibited the stimulatory effect of TGFα on DNA synthesis and cyclin D protein levels. Furthermore, knockdown of YAP1 and TAZ proteins with specific siRNAs significantly suppressed basal and TGFα-stimulated DNA synthesis and GC proliferation. The present findings in primary cultures of bovine GCs are consistent with studies in cancer cells [62–64] showing that YAP1/TAZ signaling is associated with expression
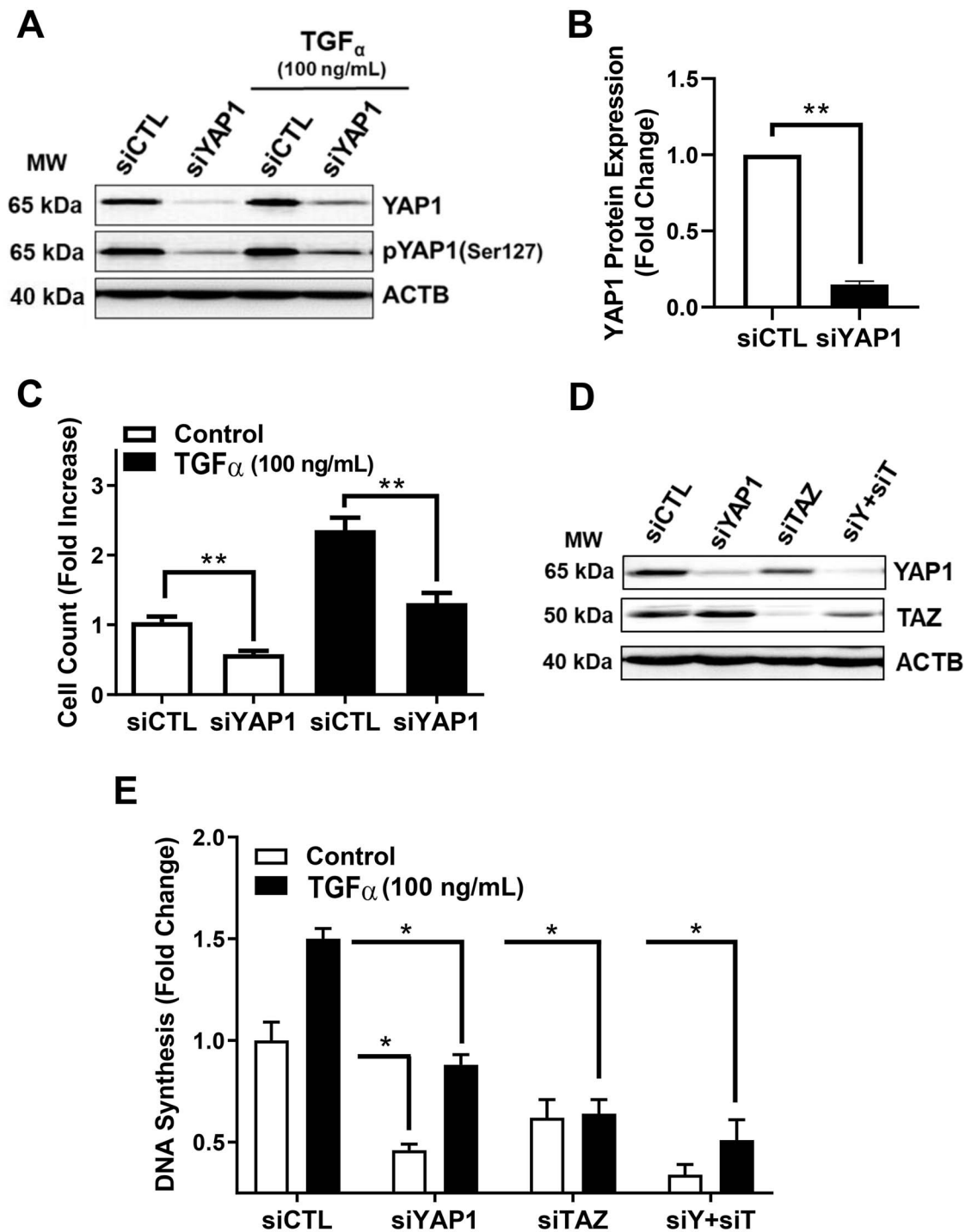
**Figure 8.** Effects of siRNA-mediated knockdown of YAP1 and TAZ on TGFα-induced proliferation in GCs. YAP1 and TAZ mRNA were silenced using siYAP1 and siTAZ in bovine GCs. Following knockdown, GCs were treated with or without transforming growth factor-alpha (50 ng/mL; TGFα) to promote cell proliferation. (A) Representative western blot showing phospho-YAP1(Ser127) and YAP1 protein expression in siGlo (siCTL) or siYAP1 knockdown GCs, following treatment with or without TGFα. (B) Densitometric analyses of YAP1 protein expression obtained from siCTL (open bars) and siYAP1 (closed bars). Bars represent means ± SEM, $n = 5$. (C) Cell counts following knockdown of YAP1 cells and treatment with TGFα (closed bars) or without TGFα (open bars). Bars are means ± SEM, $n = 3$. (D) Representative western blot showing YAP1 and TAZ protein expression in GCs following 48 h treatment with siCTL, siYAP1, siTAZ, or a combination of siYAP1 and siTAZ (siY + siT). Beta-actin (ACTB; loading control). (E) Quantitative analysis showing DNA synthesis for siCTL, siYAP1, siTAZ, or siY + siT knockdown cells treated with control (open bars) or TGFα (black bars). Data are represented as means ± SEM ($n = 3$) of the average fold change from control in each experiment. **Significant differences between treatment groups, as compared to siCTL, $P < 0.05$.
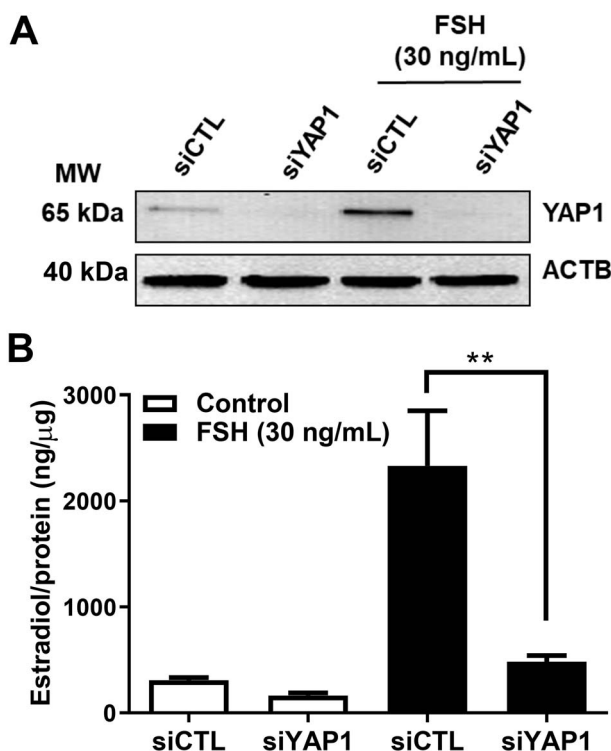
**Figure 9.** Yes-associated protein 1 is required for FSH-induced estradiol production in bovine GCs. Granulosa cells were treated with siGlo (siCTL) or siYAP1 and then treated without (control) or FSH (30 ng/ml) for 48 h prior to analysis of estradiol production. (A) Representative western blot showing YAP1 protein expression. Beta-actin (ACTB; loading control). (B) Quantitative ELISA analysis of estradiol in the culture medium. Data are represented as means $\pm$ SEM, $n = 3$. **Significant differences between treatment groups, as compared to siCTL, $P < 0.05$.

of D cyclins and progression through the G(1)/S cell cycle transition, DNA synthesis and cell proliferation. Ji et al. [26] provided evidence that the proliferation of mouse GCs in response to androgen and estrogen treatment was associated with nuclear localization of YAP1. A recent study employing microinjection of lentiviral vectors for YAP1 or siYAP1 into mouse ovaries revealed that YAP1 was required for proliferation of ovarian cells and growth of follicles [42]. This study also showed that active YAP1 signaling promoted the proliferation of mouse ovarian germline stem cells. Studies using mouse ovaries [65] and human ovarian cortex pieces [28, 66] indicate that YAP1 interacts with PI3K/AKT signaling during follicle activation. Because GCs are regulated by growth factors, gonadotropins, steroid hormones, and many other factors, it will be important to determine the signaling pathways intersecting with Hippo/YAP1 signaling that promote the proliferation of bovine GCs.

In this study, we found that Hippo/YAP1 signaling plays a role in estrogen synthesis in bovine GCs. Use of siRNA targeting YAP1 very effectively reduced FSH-stimulated production of estrogen. In a previous study, we reported that FSH-induced expression of aromatase and estrogen was blocked by knockdown of YAP1 in the human KGN GC tumor cell line [29]. These findings using an ablation approach are supported by a recent study demonstrating that microinjection of lentiviral vectors for YAP1 into mouse ovaries in vivo increased serum estrogen [42]. Additionally, Hippo core components have been reported to influence steroidogenesis in ovarian cells. For instance, an upstream negative regulator of YAP1,

SAV1, negatively regulates mRNAs associated with ovarian follicular steroidogenesis including the FSH receptor (*FSHR*) and steroidogenic acute regulatory protein (*STAR*) [25]. Studies by Pisarska [67] showed that FOXL2, a transcriptional repressor expressed GCs, is phosphorylated by LATS1; and that this phosphorylation enhances the transcriptional repression of *STAR*. Other studies indicate that YAP1 interacts with IGF1 and PI3K/AKT signaling pathways [68, 69]. Because IGF1-activated PI3K signaling contributes to aromatase expression and estrogen synthesis in ovarian cells [70–72] it seems likely that these pathways converge to elevate or stabilize CYP19A1 expression to promote estrogen synthesis. Collectively these findings suggest that Hippo signaling and its effector YAP1 may exert a key role in ovarian steroidogenesis. How Hippo signaling regulates steroidogenesis in bovine GCs is the subject of the ongoing investigation.

Following appropriate follicle development, the luteinizing hormone released from the anterior pituitary gland stimulates ovulation and causes the theca and GCs of the ovulated follicle to differentiate into small and large steroidogenic luteal cells, respectively [73–75]. The luteinized theca and GCs are unique from the undifferentiated theca and GCs in that they are fully differentiated and do not undergo cell proliferation, but rather undergo hypertrophy. We show YAP1 and TAZ are expressed in luteal tissue, including the SLCs and LLCs, but compared to the cells of the follicle, the overall protein levels of YAP1 and TAZ are reduced. In recent studies, overexpression of YAP1 was shown to induce hypertrophy in skeletal muscle fibers [76, 77], which may also be occurring in the luteal cell, due to the presence of YAP1 and TAZ in the nucleus. Evidence from studies in other systems indicates that suppression of YAP1/TAZ by mechanical cues derived from the extracellular matrix is sufficient to induce senescence and that YAP1/TAZ overexpression can overcome cell senescence [78]. It is tempting to speculate that following ovulation the mechanical microenvironment in the corpus luteum activates Hippo signaling and inhibits YAP1/TAZ, which contributes to luteal cell senescence. More work is needed to determine the role Hippo signaling plays in corpus luteum development.

Hippo signaling plays a critical role in maintaining ovarian tissue growth and homeostasis. On the contrary, disruption in Hippo signaling leads to ovarian abnormalities, tumor progression, and impaired fertility. In the normal functioning ovary, we demonstrate that Hippo signaling proteins and transcriptional co-activators, YAP1 and TAZ, are present in the bovine ovary. These Hippo signaling effectors are involved in two critical GC functions, cell proliferation, and estradiol biosynthesis, suggesting that Hippo signaling plays an important role in the development of ovarian follicles and estradiol synthesis, which are necessary for maintaining ovarian function and fertility.

## Conflict of interest

The authors have declared that no conflict of interest exists.

## Acknowledgments

# References

1. Williams CJ. Erickson GF Morphology and Physiology of the Ovary. [Updated 2012 Jan 30]. In: Feingold KR, Anawalt B, Boyce A, et al., editors. Endotext [Internet]. South Dartmouth (MA): MDText.com, Inc.; 2000-. Available from: https://www.ncbi.nlm.nih.gov/books/NBK278951/

2. Kranc W, Budna J, Kahan R, Chachuła A, Bryja A, Ciesiółka S, Borys S, Antosik M, Bukowska D, Brussow K. Molecular basis of growth, proliferation, and differentiation of mammalian follicular granulosa cells. *J Biol Regul Homeost Agents* 2017; **31**:1–8.

3. Fitzpatrick SL, Richards JS. Regulation of the rat aromatase gene in ovarian granulosa cells and R2C Leydig cells. *J Steroid Biochem Mol Biol* 1993; **44**:429–433.

4. Robker RL, Richards JS. Hormone-induced proliferation and differentiation of granulosa cells: a coordinated balance of the cell cycle regulators cyclin D2 and p27Kip1. *Mol Endocrinol* 1998; **12**:924–940v.

5. Regan SL, Knight PG, Yovich JL, Leung Y, Arfuso F, Dharmarajan A. Granulosa cell apoptosis in the ovarian follicle—a changing view. *Front Endocrinol* 2018; **9**:61.

6. Wang C, Lv X, Jiang C, Cordes CM, Fu L, Lele SM, Davis JS. Transforming growth factor alpha (TGFα) regulates granulosa cell tumor (GCT) cell proliferation and migration through activation of multiple pathways. *PLoS One* 2012; **7**:e48299.

7. Dong J, Feldmann G, Huang J, Wu S, Zhang N, Comerford SA, Gayyed MF, Anders RA, Maitra A, Pan D. Elucidation of a universal size-control mechanism in drosophila and mammals. *Cell* 2007; **130**:1120–1133.

8. Yu F-X, Guan K-L. The hippo pathway: regulators and regulations. *Genes Devel* 2013; **27**:355–371.

9. Harvey KF, Zhang X, Thomas DM. The Hippo pathway and human cancer. *Nature Rev Cancer* 2013; **13**:246–257.

10. Meng Z, Moroishi T, Mottier-Pavie V, Plouffe SW, Hansen CG, Hong AW, Park HW, Mo J-S, Lu W, Lu S. MAP 4K family kinases act in parallel to MST1/2 to activate LATS1/2 in the Hippo pathway. *Nature Coms* 2015; **6**:8357.

11. Yu F-X, Zhao B, Guan K-L. Hippo pathway in organ size control, tissue homeostasis, and cancer. *Cell* 2015; **163**:811–828.

12. Hong W, Guan K-L. The YAP and TAZ transcription co-activators: Key downstream effectors of the mammalian Hippo pathway. *Semin Cell Devel Biol, Elsevier* 2012; **23**:785–793.

13. Pobbati AV, Hong W. Emerging roles of TEAD transcription factors and its coactivators in cancers. *Cancer Biol Therap* 2013; **14**:390–398.

14. Yu F-X, Zhao B, Panupinthu N, Jewell JL, Lian I, Wang LH, Zhao J, Yuan H, Tumaneng K, Li H. Regulation of the Hippo-YAP pathway by G-protein-coupled receptor signaling. *Cell* 2012; **150**:780–791.

15. Varelas X, Miller BW, Sopko R, Song S, Gregorieff A, Fellouse FA, Sakuma R, Pawson T, Hunziker W, McNeill H. The Hippo pathway regulates Wnt/β-catenin signaling. *Dev Cell* 2010; **18**:579–591.

16. Piccolo S, Dupont S, Cordenonsi M. The biology of YAP/TAZ: Hippo signaling and beyond. *Physiol Rev* 2014; **94**:1287–1312.

17. Aragona M, Panciera T, Manfrin A, Giulitti S, Michielin F, Elvassore N, Dupont S, Piccolo S. A mechanical checkpoint controls multicellular growth through YAP/TAZ regulation by actin-processing factors. *Cell* 2013; **154**:1047–1059.

18. Boggiano JC, Fehon RG. Growth control by committee: intercellular junctions, cell polarity, and the cytoskeleton regulate Hippo signaling. *Dev Cell* 2012; **22**:695–702.

19. Mitamura T, Watari H, Wang L, Kanno H, Kitagawa M, Hassan MK, Kimura T, Tanino M, Nishihara H, Tanaka S. microRNA 31 functions as an endometrial cancer oncogene by suppressing Hippo tumor suppressor pathway. *Mol Cancer* 2014; **13**:97.

20. DiSalvo TG, Hatzopolous A, Sawyer D. TGF [beta], Wnt/[beta]-catenin and Hippo pathway" cross-talk": myocardial systems biology murmurings as the pathways converge. *British J Med Res* 2015; **6**:16–47.

21. Kawashima I, Kawamura K. Regulation of follicle growth through hormonal factors and mechanical cues mediated by Hippo signaling pathway. *Syst Biol Reprod Med* 2018; **64**:3–11.

22. Hsueh AJ, Kawamura K, Cheng Y, Fauser BC. Intraovarian control of early folliculogenesis. *Endocr Rev* 2015; **36**:1–24.

23. Xiang C, Li J, Hu L, Huang J, Luo T, Zhong Z, Zheng Y, Zheng L. Hippo signaling pathway reveals a spatio-temporal correlation with the size of primordial follicle pool in mice. *Cellular physiology and biochemistry: Int J Exp Cell Physiol Biochem Pharmacol* 2015; **35**:957–968.

24. Sun T, Pepling ME, Diaz FJ. Lats1 deletion causes increased germ cell apoptosis and follicular cysts in mouse ovaries. *Biol Reprod* 2015; **93**:22.

25. Lyu Z, Qin N, Tyasi TL, Zhu H, Liu D, Yuan S, Xu R. The Hippo/MST pathway member SAV1 plays a suppressive role in development of the prehierarchical follicles in hen ovary. *PLoS one* 2016; **11**:e0160896.

26. Ji SY, Liu XM, Li BT, Zhang YL, Liu HB, Zhang YC, Chen ZJ, Liu J, Fan HY. The polycystic ovary syndrome-associated gene Yap1 is regulated by gonadotropins and sex steroid hormones in hyperandrogenism-induced oligo-ovulation in mouse. *Mol Hum Reprod* 2017; **23**:698–707.

27. Cheng Y, Feng Y, Jansson L, Sato Y, Deguchi M, Kawamura K, Hsueh AJ. Actin polymerization-enhancing drugs promote ovarian follicle growth mediated by the Hippo signaling effector YAP. *Faseb J* 2015; **29**:2423–2430.

28. Kawamura K, Cheng Y, Suzuki N, Deguchi M, Sato Y, Takae S, Ho CH, Kawamura N, Tamura M, Hashimoto S, Sugishita Y, Morimoto Y et al. Hippo signaling disruption and Akt stimulation of ovarian follicles for infertility treatment. *Proc Natl Acad Sci USA* 2013; **110**:17474–17479.

29. Fu D, Lv X, Hua G, He C, Dong J, Lele SM, Li DW-C, Zhai Q, Davis JS, Wang C. YAP regulates cell proliferation, migration, and steroidogenesis in adult granulosa cell tumors. *Endocr-Relat Cancer* 2014; ERC-13-0339.

30. Plouffe SW, Meng Z, Lin KC, Lin B, Hong AW, Chun JV, Guan KL. Characterization of Hippo pathway components by gene inactivation. *Mol Cell* 2016; **64**:993–1008.

31. Yu C, Ji SY, Dang YJ, Sha QQ, Yuan YF, Zhou JJ, Yan LY, Qiao J, Tang F, Fan HY. Oocyte-expressed yes-associated protein is a key activator of the early zygotic genome in mouse. *Cell Res* 2016; **26**:275–287.

32. Abbassi L, Malki S, Cockburn K, Macaulay A, Robert C, Rossant J, Clarke HJ. Multiple mechanisms cooperate to constitutively exclude the transcriptional co-activator YAP from the nucleus during murine oogenesis. *Biol Reprod* 2016; **94**:102.

33. Negron-Perez VM, Hansen PJ. Role of yes-associated protein 1, angiomotin, and mitogen-activated kinase kinase 1/2 in development of the bovine blastocyst. *Biol Reprod* 2018; **98**:170–183.

34. Mao D, Hou X, Talbott H, Cushman R, Cupp A, Davis JS. ATF3 expression in the corpus luteum: possible role in luteal regression. *Mol Endocrinol* 2013; **27**:2066–2079.

35. Hou X. Arvisais E.W.. Davis J.S. Luteinizing hormone stimulates mammalian target of rapamycin signaling in bovine luteal cells via pathways independent of AKT and mitogen-activated protein kinase: modulation of glycogen synthase kinase 3 and AMP-activated protein kinase. *Endocrinology* 2010; **151**:2846–57.

36. Plewes M, Burns P. Effect of fish oil on agonist-induced receptor internalization of the PG F2α receptor and cell signaling in bovine luteal cells in vitro. *Domest Anim Endocrinol* 2018; **63**:38–47.

37. Romereim SM, Summers AF, Pohlmeier WE, Zhang P, Hou X, Talbott HA, Cushman RA, Wood JR, Davis JS, Cupp AS. Transcriptomes of bovine ovarian follicular and luteal cells. *Data Brief* 2017; **10**:335–339.

38. Romereim SM, Summers AF, Pohlmeier WE, Zhang P, Hou X, Talbott HA, Cushman RA, Wood JR, Davis JS, Cupp AS. Gene expression profiling of bovine ovarian follicular and luteal cells provides insight into cellular identities and functions. *Mole Cellu Endocrinol* 2017; **439**:379–394.

39. Sharif GM, Wellstein A. Cell density regulates cancer metastasis via the Hippo pathway. *Future Oncol* 2015; **11**:3253–3260.

40. Feng J, Gou J, Jia J, Yi T, Cui T, Li Z. Verteporfin, a suppressor of YAP-TEAD complex, presents promising antitumor properties on ovarian cancer. *Onco Targets Ther* 2016; **9**:5371–5381.

41. Wang C, Zhu X, Feng W, Yu Y, Jeong K, Guo W, Lu Y, Mills GB. Verteporfin inhibits YAP function through up-regulating 14-3-3σ sequestering YAP in the cytoplasm, American. *J Cancer Res* 2016; **6**:27–37.

42. Ye H, Li X, Zheng T, Hu C, Pan Z, Huang J, Li W, Li J, Zheng Y. The Hippo signaling pathway regulates ovarian function via the proliferation of ovarian germline stem cells. *Cell Physiol Biochem* 2017; **41**:1051–1062.

43. Sirard M-A. The ovarian follicle of cows as a model for human. *Animal Models Hum Reprod* 2017; 127–144.

44. Plouffe SW, Lin KC, Moore JL, Tan FE, Ma S, Ye Z, Qiu Y, Ren B, Guan K-LJJBC. The Hippo pathway effector proteins YAP and TAZ have both distinct and overlapping functions in the cell. *J Biol Chem* 2018; **293**:11230–11240.

45. Davis JS, Rueda BR, Spanel-Borowski KJRB. Microvascular endothelial cells of the corpus luteum. *Endocrinology*. 2003; **1**:89.

46. Talbott H, Delaney A, Zhang P, Yu Y, Cushman RA, Cupp AS, Hou X, Davis JS. Effects of IL8 and immune cells on the regulation of luteal progesterone secretion. *Reproduction* 2014; **148**:21–31.

47. Nagasawa-Masuda A, Terai KJP. Yap/Taz transcriptional activity is essential for vascular regression via CTGF expression and actin polymerization. *PlosOne* 2017; **12**:e0174633.

48. Neto F, Klaus-Bergmann A, Ong YT, Alt S, Vion A-C, Szymborska A, Carvalho JR, Hollfinger I, Bartels-Klein E, Franco CA. YAP and TAZ regulate adherens junction dynamics and endothelial cell distribution during vascular development. *Elife* 2018; **7**:e31037.

49. Park JA, Kwon Y-G. Hippo-YAP/TAZ signaling in angiogenesis. *BMB Rep* 2018; **51**:157.

50. Zhao B, Wei X, Li W, Udan RS, Yang Q, Kim J, Xie J, Ikenoue T, Yu J, Li L. Inactivation of YAP oncoprotein by the Hippo pathway is involved in cell contact inhibition and tissue growth control. *Genes Devel* 2007; **21**:2747–2761.

51. Mori M, Triboulet R, Mohseni M, Schlegelmilch K, Shrestha K, Camargo FD, Gregory RI. Hippo signaling regulates microprocessor and links cell-density-dependent miRNA biogenesis to cancer. *Cell* 2014; **156**: 893–906.

52. Wada K-I, Itoga K, Okano T, Yonemura S, Sasaki H. Hippo pathway regulation by cell morphology and stress fibers. *Development* 2011; **138**:3907–3914.

53. Fletcher GC, Elbediwy A, Khanal I, Ribeiro PS, Tapon N, Thompson BJ. The Spectrin cytoskeleton regulates the Hippo signalling pathway. *EMBO J* 2015; **34**:940–954.

54. Parker C. Essential Biological Pathways Modulate Many Different Aspects of Cell Biology. 2016:1–2. www.atlasofscience.org.

55. He C, Lv X, Hua G, Lele SM, Remmenga S, Dong J, Davis JS, Wang C. YAP forms autocrine loops with the ERBB pathway to regulate ovarian cancer initiation and progression. *Oncogene* 2015; **34**: 6040–6054.

56. Shah JS, Sabouni R, Cayton Vaught KC, Owen CM, Albertini DF, Segars JH. Biomechanics and mechanical signaling in the ovary: a systematic review. *J Assist Reprod Gene* 2018; **35**:1135–1148.

57. Wathes DC, Taylor V, Cheng Z, Mann G. Follicle growth, corpus luteum function and their effects on embryo development in postpartum dairy cows. *Reprod Suppl* 2003; **61**:219–237.

58. Skinner MK, Keski-Oja J, Osteen KG, Moses HL. Ovarian thecal cells produce transforming growth factor-β which can regulate granulosa cell growth. *Endocrinology* 1987; **121**:786–792.

59. Vendola KA, Zhou J, Adesanya OO, Weil SJ, Bondy CA. Androgens stimulate early stages of follicular growth in the primate ovary. *J Clinical Invest* 1998; **101**:2622–2629.

60. Murray A, Gosden R, Allison V, Spears N. Effect of androgens on the development of mouse follicles growing in vitro. *J Reprod Fertil* 1998; **113**:27–33.

61. Dasari VR, Mazack V, Feng W, Nash J, Carey DJ, Gogoi R. Verteporfin exhibits YAP-independent anti-proliferative and cytotoxic effects in endometrial cancer cells. *Oncotarget* 2017; **8**:28628–28640.

62. Gao Y, Shi Q, Xu S, Du C, Liang L, Wu K, Wang K, Wang X, Chang LS, He D. Curcumin promotes KLF5 proteasome degradation through downregulating YAP/TAZ in bladder cancer cells. *Internat J Mol Sci* 2014; **15**:15173–15187.

63. Chen X, Gu W, Wang Q, Fu X, Wang Y, Xu X, Wen Y. C-MYC and BCL-2 mediate YAP-regulated tumorigenesis in OSCC. *Oncotarget* 2018; **9**:668.

64. Zhang J, Wang G, Chu S-J, Zhu J-S, Zhang R, Lu W-W, Xia L-Q, Lu Y-M, Da W, Sun Q. Loss of large tumor suppressor 1 promotes growth and metastasis of gastric cancer cells through upregulation of the YAP signaling. *Oncotarget* 2016; **7**:16180.

65. Hu LL, Su T, Luo RC, Zheng YH, Huang J, Zhong ZS, Nie J, Zheng LP. Hippo pathway functions as a downstream effector of AKT signaling to regulate the activation of primordial follicles in mice. *J Cell Physiol* 2019; **234**:1578–1587.

66. Grosbois J, Demeestere I. Dynamics of PI3K and Hippo signaling pathways during in vitro human follicle activation. *Human Reprod* 2018; **33**:1705–1714.

67. Pisarska MD, Kuo FT, Bentsi-Barnes IK, Khan S, Barlow GM. LATS1 phosphorylates forkhead L2 and regulates its transcriptional activity. *Am J Physiol Endocrinol Metab* 2010; **299**:E101–E109.

68. Zhao Y, Montminy T, Azad T, Lightbody E, Hao Y, SenGupta S, Asselin E, Nicol C, Yang XJ. PI3K positively regulates YAP and TAZ in mammary tumorigenesis through multiple signaling pathways. *Mol Cancer Res* 2018; **16**:1046–1058.

69. Lin Z, Pu WT. Releasing Yap from an α-catenin trap increases cardiomyocyte proliferation. *J Cancer Res* 2015; **116**:9–11.

70. Silva J, Hamel M, Sahmi M, Price C. Control of oestradiol secretion and of cytochrome P450 aromatase messenger ribonucleic acid accumulation by FSH involves different intracellular pathways in oestrogenic bovine granulosa cells in vitro. *J Reprod* 2006; **132**:909–917.

71. Mani AM, Fenwick MA, Cheng Z, Sharma MK, Singh D, Wathes DC. IGF1 induces up-regulation of steroidogenic and apoptotic regulatory genes via activation of phosphatidylinositol-dependent kinase/AKT in bovine granulosa cells. *J Reprod* 2010; **139**:151.

72. McDonald CA, Millena AC, Reddy S, Finlay S, Vizcarra J, Khan SA, Davis JS. Follicle-stimulating hormone-induced aromatase in immature rat Sertoli cells requires an active phosphatidylinositol 3-kinase pathway and is inhibited via the mitogen-activated protein kinase signaling pathway. *J Mol Endocrinol* 2006; **20**:608–618.

73. O'Shea JD, Rodgers RJ, D'Occhio MJ. Cellular composition of the cyclic corpus luteum of the cow. *J Reprod Fertil* 1989; **85**:483–487.

74. Alila HW, Hansel W. Origin of different cell types in the bovine corpus luteum as characterized by specific monoclonal antibodies. *Biol Reprod* 1984; **31**:1015–1025.

75. Hansel W, Alila HW, Dowd JP, Milvae RA. Differential origin and control mechanisms in small and large bovine luteal cells. *J Reprod Fertil Suppl* 1991; **43**:77–89.

76. Goodman CA, Dietz JM, Jacobs BL, McNally RM, You J-S, Hornberger TA. Yes-associated protein is up-regulated by mechanical overload and is sufficient to induce skeletal muscle hypertrophy. *FEBS letters* 2015; **589**:1491–1497.

77. Watt K, Turner B, Hagg A, Zhang X, Davey J, Qian H, Beyer C, Winbanks C, Harvey K, Gregorevic P. The Hippo pathway effector YAP is a critical regulator of skeletal muscle fibre size. *Nature Comm* 2015; **6**:6048.

78. Santinon G, Brian I, Pocaterra A, Romani P, Franzolin E, Rampazzo C, Bicciato S, Dupont S. dNTP metabolism links mechanical cues and YAP/TAZ to cell growth and oncogene-induced senescence. *Embo J* 2018; **37**:e97780.